

# On the Stability, Economic Efficiency, and Incentive Compatibility of Electricity Market Dynamics

Pengcheng You, Member, IEEE, Yan Jiang, Enoch Yeung, Member, IEEE, Dennice F. Gayme, Senior Member, IEEE, and Enrique Mallada, Senior Member, IEEE

Abstract—This article studies the operation of an electricity market that accounts for participants who bid at a subminute timescale. To that end, we model the market clearing process as a dynamical system, called market dynamics, which is temporally coupled with the grid frequency dynamics and is thus required to guarantee system-wide stability while meeting operational constraints. We characterize participants as price-takers who rationally update their bids to maximize their utility in response to real-time schedules of prices and dispatch. For two common bidding mechanisms, based on quantity and price, we identify a notion of alignment between participants' behavior and a grid planner's goals, leading to a saddle-based design of market dynamics that guarantees convergence to an operating point achieving economic efficiency and incentive compatibility subject to all operational constraints. We further explore cases where this alignment property does not hold and observe that misaligned participants' bidding can destabilize the closed-loop system. We thus design a regularized version of market dynamics that recovers all the desirable stability and steady-state performance guarantees. Numerical tests validate our results on the IEEE 39-bus system.

Index Terms—Asymptotic stability, economic dispatch, frequency control, market dynamics, saddle flow dynamics.

#### I. INTRODUCTION

**E** LECTRICITY markets aim to foster competition by allowing participants to make individual bids in the market

Received 25 May 2024; revised 10 January 2025; accepted 18 April 2025. Date of publication 15 July 2025; date of current version 29 September 2025. This work was supported in part by NSFC under Grant 72201007 and Grant 72431001, in part by the NSF through CPS under Grant 2136324 and Grant 2330450, and in part by Johns Hopkins University Discovery Award and CUHKSZ University Development. An earlier version of this paper was presented in part at the ACM International Conference on Future Energy System (e-Energy 2018) [DOI: 10.1145/3208903.3208916]. Recommended by Associate Editor G. Besancon. (Corresponding author: Enrique Mallada.)

Pengcheng You is with the College of Engineering, Peking University, Beijing 100871, China (e-mail: pcyou@pku.edu.cn).

Yan Jiang is with the School of Science and Engineering, The Chinese University of Hong Kong, Shenzhen 518172, China (e-mail: yjiang@cuhk.edu.cn).

Enoch Yeung is with the Department of Mechanical Engineering, UC Santa Barbara, Santa Barbara, CA 93106 USA (e-mail: eye-ung@ucsb.edu).

Dennice F. Gayme and Enrique Mallada are with the Whiting School of Engineering, Johns Hopkins University, Baltimore, MD 21218 USA (e-mail: dennice@jhu.edu; mallada@jhu.edu).

Digital Object Identifier 10.1109/TAC.2025.3589447

clearing process [2]. With the shift of electricity generation mix toward intermittent renewables, electricity markets have to exploit resources with fast-acting capabilities to account for power balance. In order to incentivize the participation of such resources, markets, which are usually cleared at least every 5 min for economic dispatch, are required to operate at a faster, e.g., subminute, timescale. Faster market clearing provides a potential solution by 1) increasing flexibility to better accommodate the increasing system variability, and 2) increasing efficiency with finer granularity economic dispatch. However, such a fast-timescale market operation could interfere with the grid reliability, when market actions interact with the electromechanical swings of generators [3], thus raising concerns of grid operators.

Fast-timescale markets therefore have to further account for stability issues while pursuing economic efficiency. This interplay, between physics (grid dynamics) and economics (market operation), overlaps with the existing cross-timescale frequency control architectures of grid operators [4], [5]: primary—frequency regulation (tens of seconds), secondary—nominal frequency restoration (around 1 min), and tertiary—economic dispatch (at least 5 min). While there have been many recent efforts to integrate these temporally decoupled architectures, exploiting hierarchical structures and optimization decomposition across space [6], [7], [8], [9], [10], [11], [12], [13] and time [14], such approaches follow an engineering perspective and render control laws on participants that do not necessarily reflect their individual economic incentives.

Instead, in this work, we take into account participants' incentives and seek to incorporate the cross-timescale goals of frequency control in the market clearing process. In this setting, participants can bid in real time, and the market undertakes the role of ensuring economic efficiency and meeting a wide set of operational constraints (frequency regulation, power flow bounds, etc.) via pricing and dispatching. In particular, we aim to design a fast-timescale subminute market that uses market signals as control signals and thereby operates as a controller. Thus, the market rules can be seen as a dynamical system, which is usually referred to as market dynamics [3], [15], [16], [17], [18], [19]. The fundamental challenge for such a market is to simultaneously account for the physical response of the power grid and the economic incentives of its participants, e.g., generators. We model market dynamics with bids, based on quantity or price, as inputs, reflecting participants' preferences, and prices and dispatch as outputs. The market is dynamically coupled with participants (that bid according to their own preferences) and the power grid (that is constrained by Newton's and Kirchhoff's

1558-2523 © 2025 IEEE. All rights reserved, including rights for text and data mining, and training of artificial intelligence and similar technologies. Personal use is permitted, but republication/redistribution requires IEEE permission. See https://www.ieee.org/publications/rights/index.html for more information.

The notion of *market dynamics* was first introduced in [3], where a dynamic pricing signal reflecting a filtered version of system energy imbalance is proposed. Any excess (respectively, shortage) of power supplied is viewed as depressing (respectively, lifting) its value. In that setting, generators and loads respond to this signal by adjusting generation and consumption, which in turn changes the energy imbalance and thus affects the price. This work pioneered the study of the grid-marketparticipant interplay, yet it did not provide an explicit economic interpretation of this price signal and the corresponding participants' response. Since then, follow-up work has aimed at accommodating more physical constraints [15], [16], [17], including congestion management [17], as well as providing control theoretical guarantees, including delays [18] and discrete updates [19]. However, they are still predicated on the similar ad hoc designs that lack economic guarantees of efficiency and incentive compatibility.

Recently, designs for dynamic price signals, based on Lagrange dual gradient algorithms of an economic dispatch problem, have been proposed [20], [21], [22], [23]. These pricing schemes systematically embody a diverse range of operational constraints and lead to a principled design with a direct economic interpretation of equilibrium prices as well as stability guarantees. This Lagrangian-based approach further allows market participation based on both quantity [20], [21] and price bids [22], [23], e.g., raising production when prices exceed marginal costs [20], [21], or lifting prices when dispatch exceeds desired amounts [22], [23]. However, such techniques only allow for a limited homogeneous set of individual behavioral laws—mapping market outcomes to individual bid updates—that are analyzed on a case-by-case basis without systematic guarantee of incentive compatibility.

Contributions of This Work: This work builds upon recent saddle-based distributed optimization study to develop a general framework for the design and analysis of market dynamics that account for a wide range of participants' (rational) bidding behavior, market efficiency goals, and network operational constraints, while preserving system-wide stability and ensuring incentive compatibility. More precisely, we consider a setting in which participants receive price and dispatch information from the current market outcome, and seek to maximize their individual utility by updating their bids via a version of dynamic gradient play or best response.

We identify a particular notion of *alignment*, between participants' bidding behavior and a grid planner's goals, that leads to a systematic design of market dynamics. Such a design is guaranteed to drive the closed-loop system to an equilibrium that 1) is economically efficient and satisfies all operational constraints required by the grid planner, and 2) is incentive compatible with all individual participants. Our alignment condition may be satisfied even when different participants choose different update strategies. We show that this alignment condition provides a rational explanation for observations of participants' behavior in previous literature, in both quantity [3], [20], [21] and price [22] bidding settings. More specifically, we find that our alignment condition is implicitly satisfied in all of these cases. These results suggest that this framework can provide deeper understanding of previously proposed methods.

Finally, we investigate an exemplar of rational yet misaligned price bidding strategy and show that the absence of this alignment property can lead to unstable behavior. We thus propose a more robust version of the proposed market dynamics, based on regularization, which recovers asymptotic convergence and desirable steady-state performance of the closed loop. Our solution can be interpreted as an implicit regularization that aims to penalize the system misalignment, thus driving the system closer to alignment. We illustrate our results with numerical simulations on the IEEE 39-bus system.

The rest of this article is organized as follows. Section II formalizes the grid planner's goals and sets up the general framework. Section III defines the notion of alignment and characterizes the resulting systematic design of market dynamics, with application to the quantity and price bidding settings. Section IV introduces misaligned bidding behavior and highlights the required market modification to restore (approximate) alignment. Section V presents simulation results that validate the theory. Finally, Section VI concludes this article.

Notations: Let  $\mathbb{R}$ ,  $\mathbb{R}_{\geq 0}$ , and  $\mathbb{N}$  be the sets of real, nonnegative real, and natural numbers, respectively. For a finite set  $\mathcal{H} \subset \mathbb{N}$ , its cardinality is denoted as  $|\mathcal{H}|$ . For a set of scalar variables  $\{y_j, j \in \mathcal{H}\}$ , its column vector is denoted as  $y_{\mathcal{H}}$ . The subscript  $\mathcal{H}$  might be dropped if the set is clear from the context. Given vectors  $y \in \mathbb{R}^{|\mathcal{H}|}$  and  $u \in \mathbb{R}^{|\mathcal{H}|}$ ,  $y \leq u$  implies  $y_j \leq u_j \ \forall j \in \mathcal{H}$ . We define an elementwise projection  $[y]_u^{\perp}$ , where

$$[y_j]_{u_j}^+ = \begin{cases} y_j, & \text{if } y_j > 0 \text{ or } u_j > 0 \text{ holds} \\ 0, & \text{otherwise.} \end{cases}$$
 (1)

This projection is nonexpansive in the sense that for any  $u^* \ge 0$ , the following holds:

$$[y]_{u}^{+T}(u-u^{*}) \le y^{T}(u-u^{*})$$
 (2)

since the elementwise projection is active ( $[y_j]_{u_j}^+=0$ ) only with  $y_j \leq 0$  and  $u_j \leq 0$ , which still imply  $[y_j]_{u_j}^+(u_j-u_j^*)=0 \leq y_j(u_j-u_j^*)$ .

For an arbitrary matrix  $Y, Y^T$  denotes its transpose. If Y is symmetric  $(Y = Y^T)$ , we use  $Y \succeq 0, Y \succ 0, Y \preceq 0$ , and  $Y \prec 0$  to denote that Y is positive semidefinite, positive definite, negative semidefinite, and negative definite, respectively.  $Y^{-1}$  is the inverse of Y. 1 is a column vector of all 1's. In an abuse of notation, we employ 0 to denote a column vector, a row vector, or a matrix of all 0's if its dimension is clear from the context. Given a column vector of variables  $y \in \mathbb{R}^{|\mathcal{H}|}$ , we use two corresponding diagonal matrices  $\Gamma^y \in \mathbb{R}^{|\mathcal{H}| \times |\mathcal{H}|}$  and  $T^y \in \mathbb{R}^{|\mathcal{H}| \times |\mathcal{H}|}$  to denote rates of change and time constants, respectively, with  $\Gamma^y = T^{y-1}$ . Their jth diagonal elements are denoted as  $\gamma^y_j$  and  $\tau^y_j$ , respectively.

#### II. PROBLEM FORMULATION AND SETUP

We consider a continuous-time model for the interaction among grid dynamics, participants' bidding behavior, and the electricity market clearing process, i.e., *market dynamics*. We focus on the performance of this coupled system, in terms of steady-state economic dispatch and incentive compatibility, from the market perspective, and frequency stability, from the control perspective. For simplicity, we restrict active market participants to controllable generators and assume that loads are inelastic, although the framework can be extended to incorporate elastic consumers and prosumers.

In the following sections, we start with a planner's problem formulation that embodies all the target cross-timescale goals. We also set up the real-time interactive structure of the coupled system, followed by our models for rational participants' bidding.

# A. Planner's Problem

We adopt the viewpoint of a grid planner to formalize the cross-timescale economic and frequency control goals in a single problem. Consider a power network with a connected directed graph  $(\mathcal{N},\mathcal{E})$ , where  $\mathcal{N}:=\{1,2,\ldots,|\mathcal{N}|\}$  is the set of nodes and  $\mathcal{E}\subset\mathcal{N}\times\mathcal{N}$  is the set of edges connecting nodes. Each node is usually a bus, while each edge describes a connection between two buses, e.g., a transmission line. Without loss of generality, we assume there is only one (aggregate) controllable generator at each bus. We use (j,k) to denote the line from bus j to bus k. An arbitrary orientation is applied such that any  $(j,k)\in\mathcal{E}$  implies  $(k,j)\notin\mathcal{E}$ . Each line  $(j,k)\in\mathcal{E}$  is endowed with an impedance  $z_{jk}$ . We further define an incidence matrix  $C\in\mathbb{R}^{|\mathcal{N}|\times|\mathcal{E}|}$  for the network graph with its element  $C_{j,e}=1$  if  $e=(j,k)\in\mathcal{E}$  holds,  $C_{j,e}=-1$  if  $e=(k,j)\in\mathcal{E}$  holds, and  $C_{j,e}=0$ , otherwise.

We first formalize the primary and secondary control goals. Given a demand vector  $d := (d_j, j \in \mathcal{N}) \in \mathbb{R}^{|\mathcal{N}|}$ , modeled by simultaneous step change disturbances at all buses, we adopt a linearized dynamical model for the power network in transient (3a):

$$\dot{\theta} = \omega \tag{3a}$$

$$M\dot{\omega} = q - d - D\omega - CBC^T\theta \tag{3b}$$

where  $\theta := (\theta_j, j \in \mathcal{N}) \in \mathbb{R}^{|\mathcal{N}|}$  denotes bus phase angles,  $\omega := (\omega_j, j \in \mathcal{N}) \in \mathbb{R}^{|\mathcal{N}|}$  denotes bus frequencies, and q := $(q_j, j \in \mathcal{N}) \in \mathbb{R}^{|\mathcal{N}|}$  denotes generation dispatch. Here,  $M := \operatorname{diag}(M_j, j \in \mathcal{N}) \in \mathbb{R}^{|\mathcal{N}| \times |\mathcal{N}|}$  represents the generators' inertia, and  $D := \operatorname{diag}(D_i, j \in \mathcal{N}) \in \mathbb{R}^{|\mathcal{N}| \times |\mathcal{N}|}$  summarizes the generators' damping or frequency-dependent demand with  $D_i > 0$ in general.  $B := \operatorname{diag}(B_{jk}, (j, k) \in \mathcal{E}) \in \mathbb{R}^{|\mathcal{E}| \times |\mathcal{E}|}$  characterizes the sensitivity of each line flow to the phase angle difference between its two end nodes (cf., [1, Appendix] for the derivation of B). Standard assumptions are made to linearize the power flow equations in (3b): 1) bus voltage magnitudes are fixed constants, 2) lines are lossless, and 3) reactive power is ignored [24]. Note that the linearized network model (3) implicitly assumes that the variables  $\theta, \omega$ , and q, as well as the parameter d, are deviations from their steady-state nominal values prior to the imbalance caused by d. Therefore,  $\omega = 0$  represents the nominal frequency (the goal of secondary control), while  $\dot{\omega} = 0$  implies stabilized frequencies (the goal of primary control).

It will be convenient for the analysis to define  $\tilde{\theta} := C^T \theta \in \mathbb{R}^{|\mathcal{E}|}$  as the phase angle differences that determine (deviations of) line flows  $B\tilde{\theta}$  across the network, and rewrite the swing dynamics (3) in the form

$$\dot{\tilde{\theta}} = C^T \omega \tag{4a}$$

$$M\dot{\omega} = q - d - D\omega - CB\tilde{\theta}. \tag{4b}$$

We then introduce a canonical tertiary control problem that seeks to find an optimal economic dispatch of generation. At the steady state of the power network, the stationary frequencies at the nominal value, i.e.,  $\omega=0$  and  $\dot{\omega}=0$ , render (4b) a

<sup>1</sup>Note that d is unknown, but can be estimated either based on forecasts or from measurements of real-time bus net power injections  $q - d - D\omega$  [8].

characterization of the nodal power balance over the network

$$q - d - CB\tilde{\theta} = 0. \tag{5}$$

We further impose the lower and upper thermal limits  $\underline{F}$  and  $\overline{F}$  on the (deviations of) line flows:

$$F \le B\tilde{\theta} \le \overline{F}.\tag{6}$$

Then, the tertiary control (economic dispatch) problem that minimizes the aggregate generation cost to meet the demand over the network is given by

$$\min_{q,\bar{\theta}} \mathbf{1}^T J(q) \quad \text{s.t.} \quad (5), (6)$$
(7)

where  $J(q) := (J_j(q_j), j \in \mathcal{N})$  is a column vector-valued function, with  $J_j(\cdot) : \mathbb{R} \mapsto \mathbb{R}$  representing the cost function of generator j.<sup>2</sup> We assume that  $J_j(\cdot)$  is *strictly convex and twice differentiable*.

The problem (7) can be expressed compactly in terms of q by first rewriting the nodal power balance (5) in terms of the network power balance

$$\mathbf{1}^{T}\left(q-d-CB\tilde{\theta}\right) = \mathbf{1}^{T}\left(q-d\right) = 0 \tag{8}$$

where the first equality follows from  $\mathbf{1}^T C = 0$ . Then, defining the weighted *Laplacian* matrix of the power network as  $L := CBC^T$  enables (5) to be reorganized as

$$q - d = CB\tilde{\theta} = CBC^T\theta = L\theta. \tag{9}$$

The line flows  $B\dot{\theta}$  can accordingly be expressed in terms of the bus net power injections q-d

$$B\tilde{\theta} = BC^T L^{\dagger}(q - d) \tag{10}$$

where  $L^\dagger$  denotes the Moore–Penrose inverse of L. Here,  $BC^TL^\dagger$  is the power injection shift matrix of the power network. We further let  $H^T:=[(BC^TL^\dagger)^T,-(BC^TL^\dagger)^T]^T\in\mathbb{R}^{2|\mathcal{E}|\times|\mathcal{N}|}$  and  $F:=[\overline{F}^T,-\underline{F}^T]^T$  be the stacked shift matrix and thermal limit vector, respectively. The resulting equivalent reformulation of the tertiary control problem (7) is then

$$\min_{q} \quad \mathbf{1}^{T} J(q) \tag{11a}$$

s.t. 
$$\mathbf{1}^{T}(q-d) = 0 : \lambda$$
 (11b)

$$H^T(q-d) \le F : \eta \ge 0 \tag{11c}$$

where the Kirchhoff's laws are embedded in the matrix H, and  $\lambda \in \mathbb{R}$ ,  $\eta \in \mathbb{R}^{2|\mathcal{E}|}_{\geq 0}$  are the respective Lagrange dual variables for (11b) and (11c). The equivalence between the formulations (7) and (11) is formally stated below (proof by contradiction).

Lemma 1:  $q^*$  is an optimal solution to (11) if and only if  $(q^*, \tilde{\theta}^*) := C^T L^{\dagger}(q^* - d)$  is an optimal solution to (7).

The optimal primal—dual solution  $(q^*, \lambda^*, \eta^*)$  to (11) leads to an implicit definition of clearing prices based on the dual optimizers  $(\lambda^*, \eta^*)$  [14], given by the locational marginal prices (LMPs)  $\lambda^* \cdot 1 - H\eta^*$ . As guaranteed by the Karush–Kuhn–Tucker (KKT) conditions of (11), they are incentive compatible for individual generators in the sense that the clearing prices

 $<sup>^2</sup>$ Here,  $J_j(\cdot)$  is defined on the deviation of generation. For convenience of the analysis, we ignore generation capacity constraints. An alternative is to incorporate them in properly redesigned cost functions [8].

match the marginal generation costs, i.e.,  $\nabla J(q^*) = \lambda^* \cdot \mathbf{1} - H\eta^*$ , where  $\nabla J(q) := (\nabla J_j(q_j), j \in \mathcal{N})$  is a column vector-valued function of elementwise increasing gradients  $\nabla J_j(q_j)$ .

Adding now the primary and secondary control goals to the tertiary control problem leads to the following planner's problem:

Planner's problem

$$\min_{p,q,\omega,\tilde{\theta}} \quad \mathbf{1}^T J(p) + \frac{1}{2} \omega^T D\omega$$
 (12a)

s.t. 
$$q = p : \alpha$$
 (12b)

$$\mathbf{1}^T(q-d) = 0 : \lambda \tag{12c}$$

$$H^T(q-d) \le F : \eta \ge 0 \tag{12d}$$

$$q - d - D\omega - CB\tilde{\theta} = 0 : \nu \tag{12e}$$

where  $p:=(p_j,j\in\mathcal{N})\in\mathbb{R}^{|\mathcal{N}|}$  (used also to denote quantity bids) here represents more broadly individual output scheduling of generators and is required to align with market dispatch through (12b). Note that we abuse the notation to define the Lagrange dual variables  $\alpha\in\mathbb{R}^{|\mathcal{N}|}$  (used also to denote price bids),  $\lambda\in\mathbb{R},\,\eta\in\mathbb{R}^{2|\mathcal{E}|}$ , and  $\nu\in\mathbb{R}^{|\mathcal{N}|}$  for (12b)–(12e), respectively.

All the cross-timescale control goals are implicitly embedded in the optimum of the planner's problem. This fact is characterized in the following theorem (proof analogous to those of [1, Thm. 3.1 and Thm. 3.2] via analysis of the KKT conditions).

Theorem 1:  $(p^*, q^*, \omega^*, \tilde{\theta}^*)$  is an optimal solution to (12e) if and only if  $p^* = q^*$ ,  $\omega^* = 0$ , and  $\tilde{\theta}^* = C^T L^{\dagger}(q^* - d)$  hold and  $q^*$  is an optimal solution to (11).

*Corollary 1:* The optimum of the planner's problem realizes the following:

- 1) (primary control) frequency stabilization  $\dot{\omega} = 0$ , i.e., (12e);
- 2) (secondary control) the nominal frequency  $\omega^* = 0$ ;
- 3) (tertiary control) the economic dispatch  $q^*$  of (11);
- 4) (compatible participants' incentives) fully incentivized generation  $\nabla J(p^*) = \lambda^* \cdot \mathbf{1} H\eta^*$ .

The last statement follows from the KKT conditions of (12e), in particular  $\nu^* = \omega^* = 0$ . Indeed, the planner's problem (12e) suggests another way of defining clearing prices based on dual optimizers  $(\lambda^*, \eta^*, \nu^*)$ , given by  $\lambda^* \cdot \mathbf{1} - H\eta^* - \nu^*$ , such that they are incentive compatible with the economic dispatch  $q^*$ 

$$\nabla J(q^*) = \lambda^* \cdot \mathbf{1} - H\eta^* - \nu^*. \tag{13}$$

This means of pricing essentially boils down to the canonical LMPs  $\lambda^* \cdot \mathbf{1} - H\eta^*$  with  $\nu^* = 0$ .

Central to our developments will be the Lagrangian for the convex planner's problem (12e), i.e.,

$$L(p, q, \omega, \tilde{\theta}, \alpha, \lambda, \eta, \nu)$$

$$:= \underbrace{\mathbf{1}^{T} J(p)}_{\text{generators}} + \underbrace{\frac{1}{2} \omega^{T} D\omega + \nu^{T} \left( q - d - D\omega - CB\tilde{\theta} \right)}_{\text{network}}$$

$$+ \underbrace{\alpha^{T} (q - p)}_{\text{generators or market}} - \underbrace{\lambda \cdot \mathbf{1}^{T} (q - d) + \eta^{T} \left( H^{T} (q - d) - F \right)}_{\text{market}}$$

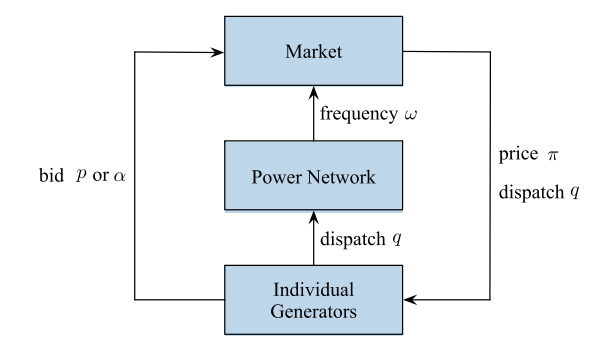


Fig. 1. Interactive structure. Only time varying exchanged information is depicted.

which we refer to as the planner's Lagrangian, with the potential responsible party for each term. It is easy to see that (14) is convex in the primal variables  $(p,q,\omega,\tilde{\theta})$  and concave (linear) in the dual variables  $(\alpha,\lambda,\eta,\nu)$ . The KKT conditions establish a bijective mapping between a min–max saddle point  $(p^*,q^*,\omega^*,\tilde{\theta}^*,\alpha^*,\lambda^*,\eta^*\geq 0,\nu^*)$  of the planner's Lagrangian (14) and an optimal primal–dual solution to the planner's problem (12e). We further refer to a function as a *reduced* planner's Lagrangian, if it is the optimum of the planner's Lagrangian (14) over a subset of the primal and dual variables.

## B. Real-Time Interactive Structure

In practice, the planner's problem (12) is not implementable due to the lack of knowledge of generators' cost functions. This poses significant challenges for the grid planner to realize economic dispatch in an incentive-compatible manner. To overcome this obstacle, we propose to use the real-time interaction among the grid, market, and participants to automatically achieve all the economic and frequency control goals. We thus consider a continuous-time setting and investigate two classes of dynamic bidding mechanisms, based on quantity and price, that allow each generator to determine its own bid while simultaneously allowing the market to update its prices and dispatch.

We propose a unified framework for the grid–market–participant loop, with a schematic layout of the interactive structure shown in Fig. 1. The power network shares real-time bus frequencies ( $\omega$ ) and (given) inelastic demand (d) with the market. The market determines the signals of clearing prices ( $\pi$ ) and generation dispatch (q) based on the network conditions and generators' bids. The bids can take the form of a quantity (p), suggesting the desired output of a generator, or a price ( $\alpha$ ), indicating the desired unit price of a generator for its output. Each individual generator responds to the market signals by implementing the prescribed dispatch<sup>3</sup> and updating its own bid to reflect its preference to the market. The dispatch immediately implemented affects the power network dynamics and may interfere with the frequency stability.

<sup>&</sup>lt;sup>3</sup>In reality, generators follow their dispatch signals subject to turbine-governor dynamics. It can be readily shown that taking into account such local dynamics does not affect the following closed-loop stability and equilibrium results [6], [7], [9], but significantly adds to difficulties in presenting the analysis. To focus on the grid–market–participant interactions here, we thus only demonstrate this point using more realistic simulation studies.

Inspired by (13) from the planner's problem (12e), we then define transient clearing prices  $\pi$  in Fig. 1 to generalize the canonical LMPs as follows.

Definition 1: Market clearing prices are defined as

$$\pi := \lambda \cdot \mathbf{1} - H\eta - \nu. \tag{15}$$

Intuitively,  $\lambda$  prices global network power imbalance,  $H\eta$  prices line congestion, and  $\nu$  prices local bus power imbalance. This dynamic version of LMPs can be interpreted as *transient shadow prices* and are bus-dependent and time-varying, embodying the sufficient control authority of the market to react to the changing network operational conditions and participants' bids.

The fundamental challenge for the coupled system in Fig. 1 to simultaneously realize the primary, secondary, and tertiary control, with a particular guarantee for compatible participants' incentives, now boils down to two problems. First, *How to characterize individual bidding behavior?* Second, *How to design market control laws of pricing and dispatch?* We aim to identify their underlying connections and address them systematically.

# C. Rational Bidding of Individual Generators

We provide a principled approach to the first problem by capturing the incentives of individual participants, which are assumed to be rational price takers. A rational generator  $j \in \mathcal{N}$  can be modeled to pursue an input–output optimization of a bidding problem, parameterized by market dispatch  $q_j$  and price  $\pi_j$  (input), which decides its bid for quantity  $p_j$  or price  $\alpha_j$  (output). Therefore, we formulate a general form of the bidding problem for each generator j as

Individual generator bidding problem

Input: clearing price  $\pi$  and dispatch q; output: bid  $p, \alpha$ 

$$\max_{p_j} \quad U_j(p_j; q_j, \pi_j) \tag{16a}$$

s.t. 
$$G_j(p_j; q_j, \pi_j) = 0 : \alpha_j$$
 (16b)

where  $U_j(\cdot)$  and  $G_j(\cdot)$  are, respectively, real-valued concave and convex functions to represent the objective and constraint of generator  $j.^4$  We use the dual variable  $\alpha_j$ , a proxy for the marginal cost, as the price bid. We will provide more intuitions later. Note that only one type of bid p or q will be present. We adopt a gradient-based methodology to characterize the rational bidding behavior of individual generators. To solve the bidding problem (16), we define its Lagrangian  $L_j(p_j, \alpha_j; q_j, \pi_j)$  and choose between

$$\dot{p}_j = \gamma_j^p \cdot \nabla_{p_j} L_j$$
 (respectively,  $\dot{\alpha}_j = -\gamma_j^\alpha \cdot \nabla_{\alpha_j} L_j$ )
(17a)

$$p_j = \arg\max_{p_j} L_j \quad (\text{respectively, } \alpha_j = \arg\min_{\alpha_j} L_j) \quad (17b)$$

as the individual dynamic gradient play [25] or best response for bidding. We will discuss next the explicit formulations of the bidding problem (16) and the resulting bidding behavior, and further develop the countermeasure of market control laws to address the second problem.

#### III. ALIGNED MARKET DYNAMICS

In this section, we develop a systematic design of market dynamics that is able to accommodate a family of participants' bidding behavior, referred to as *aligned bidding*. The design is inspired by a formulation of a network problem based on the swing dynamics (4) as well as its connection with the planner's Lagrangian (14). We will first characterize the general paradigm of alignment, and then showcase two specific examples of such market dynamics designs from existing literature.

### A. Network Problem

We first formulate a network problem that implicitly embodies the physical swing dynamics (4)

Network problem

Input: dispatch q; output: frequency  $\omega$ 

$$\min_{\omega,\tilde{\theta}} \quad \frac{1}{2}\omega^T D\omega \tag{18a}$$

s.t. 
$$q - d - D\omega - CB\tilde{\theta} = 0 : \nu$$
. (18b)

By defining its Lagrangian

$$L_n(\omega, \tilde{\theta}, \nu) := \frac{1}{2}\omega^T D\omega + \nu^T (q - d - D\omega - CB\tilde{\theta})$$
 (19)

we can express the swing dynamics (4) as

$$\omega = \arg\min_{n} L_n \tag{20a}$$

$$\dot{\tilde{\theta}} = -\Gamma^{\tilde{\theta}} \nabla_{\tilde{\theta}} L_n \tag{20b}$$

$$\dot{\nu} = \Gamma^{\nu} \nabla_{\nu} L_n \tag{20c}$$

with  $\Gamma^{\tilde{\theta}}=B^{-1}$  and  $\Gamma^{\nu}=M^{-1}$ . Note that (20a) enforces  $\omega\equiv\nu$  even in transient, which allows us to use  $\omega\leftrightarrow\nu$  interchangeably. Therefore, the clearing prices  $\pi$  in (15) are equivalently  $\pi=\lambda\cdot 1-H\eta-\omega$ .

Note that the network problem (18) can be viewed as part of the planner's problem (12e). More formally, we define an *aligned* relation between the network and the grid planner as follows.

Definition 2: The power network dynamics (4) are aligned with the grid planner's goals in the sense that

$$\nabla_u L_n = \nabla_u L \tag{21}$$

holds for the network variables  $u = \omega, \hat{\theta}, \nu$ .

The alignment (21) means that (20) can be equivalently expressed in terms of the planner's Lagrangian L in (14). It further implies that the physical response of the power network automatically implements a partial saddle flow (21) of L or its possibly reduced variant. Similar interpretations are identified in [6], [7], [8], [9], and [10]. Since the network chooses (20a) for  $\omega$  (reduction), we accordingly define a reduced planner's Lagrangian

$$\bar{L}(p,q,\tilde{\theta},\alpha,\lambda,\eta,\nu) \; := \; \min_{\omega} \; L(p,q,\omega,\tilde{\theta},\alpha,\lambda,\eta,\nu). \quad (22)$$

## B. Aligned Bidding and Market Dynamics Design

We model the individual bidding behavior of generator  $j \in \mathcal{N}$  by the dynamic gradient play or best response in (17) with respect to the Lagrangian  $L_j$  of its bidding problem. In light of the same gradient-based structure as (21), a particular family

<sup>&</sup>lt;sup>4</sup>Equation (16b) only involves equality constraints in our work. However, it can easily generalize to inequality constraints.

of participants' behavior is identified to satisfy the following notion of alignment.

Definition 3: Individual generators' bidding behavior is aligned with the grid planner's goals if

$$\nabla_u L_j = \nabla_u \tilde{L} \tag{23}$$

holds for the bidding variables  $u = p_i, \alpha_i$ , where  $\tilde{L}$  is a possibly reduced variant of L in (22).

We will make the following assumption on L.

Assumption 1:  $\tilde{L}$ , as well as all other possibly reduced variants of  $\bar{L}$ , is finite in any bounded region of its domain.

Remark 1: With some particular reduction,  $\tilde{L}$  may always attain infinity and is thus not well defined. Assumption 1 excludes such L's from consideration. Such circumstances are common, especially when the planner's Lagrangian L is linear with respect to the variables to be optimized. However, it is possible to circumvent the issue by introducing an additional regularization term of the form  $||x - \hat{x}||^2$ , with  $\hat{x}$  being an auxiliary variable, whenever optimizing  $\bar{L}$  over x alone leads to infinity [26], [27]. Therefore, we implicitly assume that all the reduced Lagrangians discussed later are well defined.

This alignment between participants and the grid planner in Definition 3 also connects the way each individual participant bids (17) with a partial saddle flow of L (or its possibly reduced variant), in addition to (21) realized by the swing dynamics (4). Note that the saddle points of the planner's Lagrangian L in (14), and thus also L, optimally solve the planner's problem (12e) and achieve all of its goals. This connection inspires a design of aligned market dynamics that complements the saddle flow through pricing and dispatch.

In general, with either dynamic bidding mechanism of quantity p or price  $\alpha$ , the market seeks to solve an input–output variant of the planner's problem (12e), where some quantities, e.g., bids and frequencies, are assumed as given (input), and prices and dispatch are to be computed and released to participants (output). We formulate such a problem in a generic form as follows:

Market problem<sup>5</sup>

Input: bid  $\alpha$ , p and frequency  $\omega$ ; output: clearing price  $\pi$  and dispatch q

$$\min_{q} \quad U_m(q; p, \alpha, \omega) \tag{24a}$$

s.t. 
$$G_m(q; p, \alpha, \omega) \le 0 : (\lambda, \eta \ge 0)$$
 (24b)

where  $U_m(\cdot)$  and  $G_m(\cdot)$  are real-valued and vector-valued convex functions that, respectively, represent the market objective and constraints. Note that the general expression describing inequality constraints also captures equality constraints. We could also develop gradient-based market control laws for pricing and dispatch that can be interpreted as a primal-dual algorithm to solve the market problem (24). In particular, we define for the market problem (24) its Lagrangian  $L_m(q, \lambda, \eta; p, \alpha, \omega)$  and likewise choose between

$$\dot{u} = -\Gamma^u \nabla_u L_m$$
 (respectively,  $\dot{u} = \Gamma^u \left[ \nabla_u L_m \right]_{\eta}^+$ ) (25a)

$$\dot{u} = -\Gamma^u \nabla_u L_m$$
 (respectively,  $\dot{u} = \Gamma^u \left[ \nabla_u L_m \right]_{\eta}^+$ ) (25a)  
 $u = \arg\min_u L_m$  (respectively,  $u = \arg\max_{u:\eta \ge 0} L_m$ ) (25b)

for any primal variable u = q (respectively, dual variables u = $\lambda, \eta$ ) to solve for the optimal value. The projection  $[\cdot]_{\eta}^{+}$  applies only to  $u = \eta$ , which guarantees that the trajectory of  $\eta(t)$ starting from an arbitrary nonnegative point remains nonnegative. Given the alignment of both the power network (21) and participants (23), the key design is to exploit L and the choice of participants' bidding update (dynamic gradient play or best response) in (17), and extract the corresponding market problem (24) from the planner's problem (12e). In particular, suppose Lis the optimum of  $\bar{L}$  over a subset of variables  $v_m$ , i.e.,  $L = \bar{L}|_{v_m^*}$ with  $v_m^*$  being the optimizer, and a subset  $\bar{\mathcal{N}} \subset \mathcal{N}$  of generators use (17b) to bid  $v_{\bar{N}}$ —also a subset of variables of  $\bar{L}$ . We propose to design the market such that the following holds.

1) For the market variables  $u = q, \lambda, \eta$ 

$$\nabla_u L_m = \nabla_u \bar{L}|_{v_{\pi}^*} \tag{26}$$

holds (thus also aligned), where  $v_{\tilde{\mathcal{N}}}^*$  is the optimizer;

2) Equation (25b) is chosen for  $v_m$  to yield L in (23).

Based on the bidding mechanism, we can always apply optimization decomposition to the planner's problem (12e) to obtain the desired market problem (24) (see examples in Section II-I-C). By this means, the market control laws (25) are basically designed to complement the saddle flow of a particular reduced planner's Lagrangian that accounts for all the reduced parts, given by

$$\hat{L} := \bar{L}|_{v_m^*, v_{sr}^*}. (27)$$

Such aligned market dynamics render the joint dynamics of the grid, market, and participants a (projected) saddle flow of  $\tilde{L}$ . Thus, the grid-market-participant loop can be expressed as

$$\begin{bmatrix} T^z & \\ & T^\sigma \end{bmatrix} \begin{bmatrix} \dot{z} \\ \dot{\sigma} \end{bmatrix} = \begin{bmatrix} -\nabla_z \hat{L}(z, \sigma) \\ \left[\nabla_\sigma \hat{L}(z, \sigma)\right]_\eta^+ \end{bmatrix}$$
(28)

where z and  $\sigma$  are, respectively, the subsets of the primal variables  $(p, q, \theta)$  and the dual variables  $(\alpha, \lambda, \eta, \nu)$ , which are updated using the gradient information via (17a), (20b), (20c), and (25a). We slightly abuse the notation such that the projection  $[\cdot]_{\eta}^{+}$  only applies to part of the gradient corresponding to  $\eta$  in  $\sigma$ . The remaining variables are updated based on (17b), (20a), and (25b).

To gain insights into this closed-loop interaction (28), we next show that its equilibria correspond to optimal solutions to the planner's problem (12e). We further show that it converges asymptotically to one such equilibrium point under mild conditions. If  $\eta$  is contained in  $\sigma$ , define

$$\mathbb{I} := \left\{ (z, \sigma) \mid \eta \in \mathbb{R}^{2|\mathcal{E}|}_{\geq 0} \right\}$$
 (29)

as the set of initial points in order to guarantee a nonnegative trajectory for  $\eta$ ; otherwise, define  $\mathbb{I} := \mathbb{R}^{|z|+|\sigma|}$ . Then, the equilibria of the grid-market-participant loop (28) can be characterized by the following theorem (proof in Appendix A).

Theorem 2: Let Assumption 1 hold. For the grid-marketparticipant loop (28), a point  $(z^*, \sigma^*) \in \mathbb{I}$  is an equilibrium if and only if  $(z^*, \sigma^*)$  corresponds to an optimal primal–dual solution to the planner's problem (12).

Theorem 2 indicates that each equilibrium point not only restores the nominal frequency, but also achieves underlying

<sup>&</sup>lt;sup>5</sup>Since only one of  $\alpha$  and p will serve as bids and the input for the market problem, as we will see later,  $\alpha$  may be included in the market variables in the quantity bidding case. However, it will not affect the market output.

economic dispatch—demand met in an economically efficient manner and line thermal limits respected—while fulfilling compatible participants' incentives through individual bidding.

We proceed to show the convergence of the closed-loop system (28) to one equilibrium point. Given the initial condition of  $\mathbb{I}$ , define

$$\mathbb{E} := \{ (z, \sigma) \mid \dot{z} = 0, \dot{\sigma} = 0 \} \tag{30}$$

as the set of its equilibrium points. We make the following assumption on the system observability that leads to the asymptotic stability of the equilibrium set described in Theorem 3 (proof in Appendix B).

Assumption 2 (Observability): The grid–market–participant loop (28) has an observable output  $\hat{L}(z,\sigma)$  such that for any of its trajectories  $(z(t),\sigma(t))$  that satisfies  $\hat{L}(z^*,\sigma(t)) \equiv \hat{L}(z^*,\sigma^*)$  and  $\hat{L}(z(t),\sigma^*) \equiv \hat{L}(z^*,\sigma^*)$ , we have  $\dot{z} \equiv 0$  and  $\dot{\sigma} \equiv 0$ .

Theorem 3: If Assumptions 1 and 2 hold, then the equilibrium set  $\mathbb{E}$  is globally asymptotically stable on  $\mathbb{I}$ . In particular, starting from any initial point in  $\mathbb{I}$ , a trajectory  $(z(t), \sigma(t))$  of the grid—market–participant loop (28) remains bounded for  $t \geq 0$  and converges to  $(z^*, \sigma^*)$  with  $t \to \infty$ , where  $(z^*, \sigma^*)$  is one specific equilibrium point in  $\mathbb{E}$ .

Assumption 2 is a weaker version of the classical observability notion that exploits the saddle-point properties of the planner's Lagrangian (14) [27]. It essentially entails particular structures for  $L(z,\sigma)$ , or the planner's problem (12). Note that  $\hat{L}(z(t), \sigma(t)) \equiv \hat{L}(z^*, \sigma^*) \Rightarrow (z(t), \sigma(t)) \equiv (z^*, \sigma^*)$  does not suffice for an observable output in this case. Theorem 3 implies that, under mild conditions, the aligned participants' bidding behavior together with the proposed market dynamics can essentially function as a feedback controller on the power network dynamics to simultaneously realize the cross-timescale primary, secondary, and tertiary control with compatible participants' incentives. Note that similar to nominal frequency restoration, economic efficiency with congestion management and incentive compatibility are both steady-state requirements. They are achieved at any equilibrium point  $(z^*, \sigma^*)$  of the grid-market-participant loop (28), as suggested by Theorem 2. Indeed, this notion of alignment establishes connections to the rationale of saddle flow dynamics [26], [27], [28] that underlies such principled grid-market-participant loop (28). As a result, the rate of convergence could also be analyzed—see an example in [29], although it is not pursued here.

#### C. Illustrative Examples

We next present two examples of aligned market dynamics, based on the two common bidding mechanisms of quantity and price, respectively. The two examples take root in existing literature [1], [21], [22]. For illustration purposes, we follow a uniform choice of bidding behavior [either (17a) or (17b) for all participants] as in [1] and [21]. We note, however, the results presented in this article can accommodate mixed choices, thus generalizing previous works. We also show through the examples that the observability condition in Assumption 2 is readily satisfied for the grid—market—participant loop (28).

1) Quantity Bidding: The quantity bidding mechanism allows individual generator participants to bid their own decisions on the amount of electricity generation p into the market. All the received quantity bids p are respected and taken as the generation dispatch q. However, the market aims to match the supply with

given demand and meet the network operational constraints by setting appropriate clearing prices  $\pi$  to coordinate these quantity bids.

Since the dispatch  $q_j$  of generator j follows its quantity bid  $p_j$ , it is able to maximize its profit from the market, given the clearing price  $\pi_j$  at bus  $j \in \mathcal{N}$ , by solving its bidding problem

$$U_j(p_j; \pi_j) := \pi_j p_j - J_j(p_j)$$
 (31a)

$$G_j(p_j; \pi_j) = 0 \quad : \quad \varnothing. \tag{31b}$$

The unconstrained problem  $(31)^6$  immediately suggests

$$L_i(p_i; \pi_i) := \pi_i p_i - J_i(p_i)$$
 (32)

and the dynamic gradient play of (17a) on  $p_j$  gives the bidding strategy of generator j [1], [21]

$$\tau_i^p \dot{p}_i = \pi_i - \nabla J_i(p_i) \quad j \in \mathcal{N}. \tag{33}$$

Note that (33) reveals a direct economic interpretation that generator j tends to augment production  $p_j$  if the offered clearing price  $\pi_j$  exceeds its marginal cost  $\nabla J_j(p_j)$ ; otherwise, it will curtail production  $p_j$ . It is therefore incentivized to adapt its production  $p_j$  in a way that matches its marginal cost  $\nabla J_j(p_j)$  with the clearing price  $\pi_j$ , which will bring it the maximum profit. Equation (33) represents exactly the rational quantity bidding behavior of a price-taking generator.

Further, (33) satisfies the alignment condition in Definition 3 based on the following reduced planner's Lagrangian:

$$\tilde{L}(p,\tilde{\theta},\lambda,\eta,\nu) := \min_{q} \max_{\alpha} \ \bar{L}(p,q,\tilde{\theta},\alpha,\lambda,\eta,\nu) \tag{34}$$

which leads to  $q \equiv p$  even in transient, i.e., dispatch follows quantity bids, exactly as the bidding mechanism mandates.

Given (33) and (34), in this case,  $v_m$  contains q and  $\alpha$ , while  $v_{\bar{\mathcal{N}}}$  is  $\varnothing$ . Based on (26), we aim for  $L_m$  such that  $\nabla_u L_m = \nabla_u \bar{L}$  holds for  $u=q,\lambda,\eta$ . Note that now the market enforces q=p. Then, by inheriting all the market-related terms (independent of  $\omega$ ) from the planner's Lagrangian (14), we obtain  $L_m$  as

$$L_m(q, \alpha, \lambda, \eta; p) := \alpha^T(q - p) - \lambda \cdot \mathbf{1}^T(q - d) + \eta^T \left( H^T(q - d) - F \right). \tag{35}$$

Note that here  $\alpha$  is a market dual variable. Equation (35) implies the explicit market problem formulation (24) as

$$U_m(q;p) := 0 (36a)$$

$$G_m(q;p) \le 0$$
 : (12b)-(12d). (36b)

The market problem (36) is a feasibility problem that coordinates quantity bids of individual generation scheduling through pricing ( $\pi = \lambda \cdot \mathbf{1} - H\eta - \omega$ ). We need to further select (25a) for  $(\lambda, \eta)$  and (25b) for  $(q, \alpha)$  [to yield  $\tilde{L}$  in (34)]. The resulting formal aligned market dynamics are

$$q \equiv p$$
 (37a)

$$T^{\lambda}\dot{\lambda} = -\mathbf{1}^{T}(q-d) \tag{37b}$$

$$T^{\eta}\dot{\eta} = \left[H^T(q-d) - F\right]_{\eta}^+. \tag{37c}$$

Under the quantity bidding mechanism, the grid-market-participant loop, consisting of (4), (33), and (37), equivalently

<sup>&</sup>lt;sup>6</sup>We use the empty set symbol  $\varnothing$  to refer to the lack of constraints.

implements the projected saddle flow (28) of the underlying reduced planner's Lagrangian  $\hat{L} = \tilde{L}$  in (34) that optimizes  $\bar{L}$  over  $(v_m, v_{\bar{N}})$ , i.e.,

$$\hat{L}(z,\sigma) := \min_{q} \max_{\alpha} \ \bar{L}(p,q,\tilde{\theta},\alpha,\lambda,\eta,\nu)$$
 (38)

with  $z := (p, \tilde{\theta}) \in \mathbb{R}^{|\mathcal{N}| + |\mathcal{E}|}$  and  $\sigma := (\lambda, \eta, \nu) \in \mathbb{R}^{|\mathcal{N}| + 2|\mathcal{E}| + 1}$ . In this setting, the observability in Assumption 2 indeed holds as claimed below (proof in Appendix C).

Proposition 1: Given  $\hat{L}(z,\sigma)$  in (38), if any trajectory  $(z(t),\sigma(t))$  of the grid–market–participant loop (28) satisfies  $\hat{L}(z^*,\sigma(t)) \equiv \hat{L}(z^*,\sigma^*)$  and  $\hat{L}(z(t),\sigma^*) \equiv \hat{L}(z^*,\sigma^*)$ , then  $\dot{z} \equiv 0$  and  $\dot{\sigma} \equiv 0$  hold.

2) Price Bidding: The price bidding mechanism allows individual generator participants to bid into the market the desired prices  $\alpha$  of electricity at which they are willing to sell. Such a price bid is expected to implicitly reflect the marginal generation cost without revealing a generator's truthful cost function. The market targets an economic schedule of generation dispatch q with the corresponding incentive compatible clearing prices  $\pi$  based on these price bids.

Given the market dispatch  $q_j$  and clearing price  $\pi_j$  at bus  $j \in \mathcal{N}$ , generator j is obliged to follow the designated generation dispatch but still can strive for profit maximization through its price bid:

$$U_j(p_j; q_j, \pi_j) := \pi_j q_j - J_j(p_j)$$
 (39a)

$$G_i(p_i; q_i, \pi_i) = 0$$
 : (12b). (39b)

We interpret the price bid from the dual perspective and define a corresponding Lagrangian  $L_i$ 

$$L_i(p_i, \alpha_i; q_i, \pi_i) := \pi_i q_i - J_i(p_i) + \alpha_i (p_i - q_i).$$
 (40)

We adopt (17a) for  $\alpha$  and (17b) for p to characterize the bidding strategy of generator j [22]

$$\tau_j^{\alpha} \dot{\alpha}_j = q_j - (\nabla J_j)^{-1} (\alpha_j) \quad j \in \mathcal{N}$$
 (41)

where we have substituted  $p_j=(\nabla J_j)^{-1}(\alpha_j)$  from (17b) for p. The rational bidding behavior (41) reveals generator j's effort to align its desired generation  $(\nabla J_j)^{-1}(\alpha_j)$ , conveyed through the price bid  $\alpha_j$ , with the given dispatch  $q_j$ . For example, an increase in  $\alpha_j$  implies raised desired generation  $(\nabla J_j)^{-1}(\alpha_j)$  (by convexity), and meanwhile signals the market to decrease the corresponding dispatch  $q_j$ , thus diminishing the gap in between. It can be readily verified that (41) also satisfies Definition 3 of alignment with  $\tilde{L}=\bar{L}$  in (22). Therefore,  $v_m$  is  $\varnothing$ , while we have  $v_{\bar{N}}=p$ , from (41). Based on (26), we aim for  $L_m$  such that  $\nabla_u L_m = \nabla_u \min_p \bar{L}$  holds for  $u=q,\lambda,\eta$ . Note that now p=q is accounted for by individual generators in (39b). Then, inheriting all the market-related terms (independent of p) from the planner's Lagrangian (14), including  $v^Tq$  and  $\alpha^Tq$  that capture interactions, leads to

$$L_m(q, \lambda, \eta; \alpha, \omega) := (\alpha + \omega)^T q - \lambda \cdot \mathbf{1}^T (q - d) + \eta^T (H^T (q - d) - F)$$
(42)

with interchangeable  $\omega \leftrightarrow \nu.$  It corresponds to the desired market problem as

$$U_m(q;\alpha,\omega) := (\alpha+\omega)^T q$$
 (43a)

$$G_m(q; \alpha, \omega) \le 0$$
 : (12c)-(12d). (43b)

The market problem (43) uses the price bids and the frequencies,  $\alpha + \omega$ , as a proxy for the unit generation costs, and minimizes the corresponding aggregate generation cost—a frequency-aware variant of economic dispatch. Since  $v_m$  is  $\varnothing$ , we will just implement (25a) for  $(q, \lambda, \eta)$ , leading to the formal aligned market dynamics:

$$T^q \dot{q} = \lambda \cdot \mathbf{1} - H\eta - \omega - \alpha \tag{44a}$$

$$T^{\lambda}\dot{\lambda} = -\mathbf{1}^{T}(q-d) \tag{44b}$$

$$T^{\eta}\dot{\eta} = \left[H^T(q-d) - F\right]_{\eta}^+. \tag{44c}$$

Under the price bidding mechanism, the grid-market-participant loop, consisting of (4), (41), and (44), equivalently implements the projected saddle flow (28) of the underlying reduced planner's Lagrangian

$$\hat{L}(z,\sigma) := \min_{p} \ \bar{L}(p,q,\tilde{\theta},\alpha,\lambda,\eta,\nu) \tag{45}$$

based on (27), with  $z:=(q,\tilde{\theta})\in\mathbb{R}^{|\mathcal{N}|+|\mathcal{E}|}$  and  $\sigma:=(\alpha,\lambda,\eta,\nu)\in\mathbb{R}^{2|\mathcal{N}|+2|\mathcal{E}|+1}$ . Here,  $p\equiv(\nabla J)^{-1}(\alpha)$  is enforced with the column vector-valued inverse function  $(\nabla J)^{-1}(\alpha):=((\nabla J_j)^{-1}(\alpha_j),j\in\mathcal{N})$  representing the elementwise inverse of gradients. The observability in Assumption 2 likewise holds here as formally stated below (proof analogous to that of Proposition 1).

*Proposition 2:* Given  $\hat{L}(z,\sigma)$  in (45), if any trajectory  $(z(t),\sigma(t))$  of the grid–market–participant loop (28) satisfies  $\hat{L}(z^*,\sigma(t)) \equiv \hat{L}(z^*,\sigma^*)$  and  $\hat{L}(z(t),\sigma^*) \equiv \hat{L}(z^*,\sigma^*)$ , then  $\dot{z} \equiv 0$  and  $\dot{\sigma} \equiv 0$  hold.

# IV. MISALIGNED MARKET DYNAMICS

In general, individual participants are not obliged to conform with any behavior pattern aligned with the market. If they do not bid in an aligned manner, the role of market dynamics has to be reevaluated. In this section, we propose an exemplar of rational price bidding strategy for price-taking participants that is misaligned. To maintain the desirable properties of the market dynamics, a modification on the market control laws is necessary to accommodate the misalignment.

### A. Misaligned Price Bidding

We still consider the dynamic price bidding mechanism where each generator j interacts with the market through its price bid  $\alpha_j$ . From a generator's perspective, given the market dispatch  $q_j$  and clearing price  $\pi_j$ , one alternative to fully exploit the market information is to check whether the pair  $(q_j, \pi_j)$  satisfies incentive compatibility, i.e., whether its marginal generation cost matches the clearing price,  $\nabla J_j(q_j) = \pi_j$ . Note that

$$(\nabla J_j)^{-1}(\pi_j) = \arg\max_{p_j} \pi_j p_j - J_j(p_j)$$
 (46)

is indeed the individual desired generation that maximizes generator j's profit given the clearing price  $\pi_j$ . If it is matched by the market dispatch  $q_j$ , the generator should be satisfied with its current clearing price and dispatch. Otherwise, any discrepancy between the individual desired generation and the

<sup>7</sup>The linear programming formulation (43) may not be well defined (finite optimum) in general without generation capacity constraints. However, it is sufficient to derive control laws that make the closed loop steady-state optimal.

market dispatch would drive generator j to strive for compatible incentives.

This idea inspires a new formulation of the individual price bidding problem

$$U_j(p_j;q_j,\pi_j) \quad := \quad 0 \tag{47a}$$

$$G_j(p_j; q_j, \pi_j) = 0t$$
 : 
$$\begin{cases} (12b) \\ p_j = (\nabla J_j)^{-1}(\pi_j) \end{cases}$$
 (47b)

where (47b) still enforces the market dispatch  $q_j$  to be strictly followed while generator j requires it to be incentive compatible with the clearing price  $\pi_j$ . This is a feasibility problem and we still interpret the price bidding from the dual perspective. We define  $L_j$  to be a partial Lagrangian of (47) that only relaxes (12b)

$$L_j(\alpha_j; q_j, \pi_j) := \alpha_j \left( (\nabla J_j)^{-1} (\pi_j) - q_j \right)$$
 (48)

where we have plugged in  $p_j = (\nabla J_j)^{-1}(\pi_j)$  to indicate the individual desired generation. The dynamic gradient play (17a) on  $\alpha$  defines an alternative price bidding strategy for generator j

$$\tau_i^{\alpha} \dot{\alpha}_j = q_j - (\nabla J_j)^{-1}(\pi_j) \quad j \in \mathcal{N}. \tag{49}$$

Compared with the previous aligned bidding behavior (41), the clearing price information is exploited here instead of each local bid. To some extent, the current strategy (49) is even more straightforward and compelling for rational individual generators since it directly reflects their economic incentives. For instance, if a generator is dispatched more than its desired generation, it raises its price bid to indicate more costly production in anticipation of a reduced dispatch or a lifted clearing price, at which it is willing to produce more. The price bid  $\alpha_j$  will remain fixed only when the pair of the market dispatch  $q_j$  and clearing price  $\pi_j$  satisfies  $\nabla J_j(q_j) = \pi_j$  to be incentive compatible. Note that a generator bidding according to (49) is still a price-taker since it just responds to the given dispatch and clearing price.

Suppose the market still maintains the market control laws (44), attained from the market problem (43) under the price bidding mechanism. The alignment condition does not hold here since there does not exist any reduced planner's Lagrangian that satisfies Definition 3. In fact, the insertion of  $p = (\nabla J)^{-1}(\pi)$  into the planner's Lagrangian (14) could deprive it of the concavity in the dual variables  $(\alpha, \lambda, \eta, \nu)$ . The next illustrative example further suggests that such misalignment can lead to system instability.

Single-bus example: We adopt a quadratic form for  $J_i(\cdot)$ 

$$J_j(q_j) := \frac{c_j}{2} q_j^2 + \bar{c}_j q_j \tag{50}$$

which is parameterized by constants  $c_j > 0$  and  $\bar{c}_j$ . Consider the following illustrative single-bus example. Ignoring the states  $\tilde{\theta}$  and  $\eta$  (no network), dropping subscripts, and setting  $M = D = T^{\alpha} = T^q = T^{\lambda} = c = \bar{c} = 1$  give the following dynamics:

$$\begin{bmatrix} \dot{\omega} \\ \dot{\alpha} \\ \dot{q} \\ \dot{\lambda} \end{bmatrix} = \underbrace{\begin{bmatrix} -1 & 0 & 1 & 0 \\ 1 & 0 & 1 & -1 \\ -1 & -1 & 0 & 1 \\ 0 & 0 & -1 & 0 \end{bmatrix}}_{=:A} \begin{bmatrix} \omega \\ \alpha \\ q \\ \lambda \end{bmatrix} + \underbrace{\begin{bmatrix} -d \\ 1 \\ 0 \\ d \end{bmatrix}}_{\text{constant}}.$$
 (51)

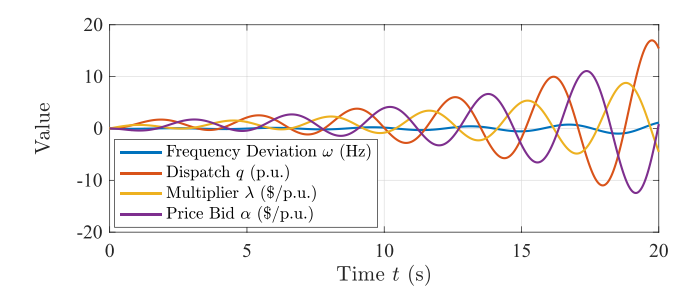


Fig. 2. Simulation run of illustrative example (51).

It can be checked that the matrix A has a pair of complex-conjugate eigenvalues  $0.16 \pm i1.75$  with positive real parts. Thus, the system (51) is not stable, as also illustrated in Fig. 2.

The example indicates that individual participants being rational price-takers is not sufficient to guarantee alignment between participants and the grid planner. Further, such misalignment can render the design of saddle-based market dynamics (44) closed-loop unstable. The source of the misalignment in this case can be understood as having participants' bidding dynamics based on saddle flows of different reduced Lagrangians.

More precisely, for the closed-loop system (4), (44), and (49), one can identify that individual participants choose the desired generation  $p^{\ddagger}$  from the following reduced planner's Lagrangian:

$$p^{\ddagger} := \arg\min_{p} \left\{ \max_{\alpha} \min_{q} \ \bar{L}(p, q, \tilde{\theta}, \alpha, \lambda, \eta, \nu) \right\}$$
$$= (\nabla J)^{-1} (\lambda \cdot \mathbf{1} - H\eta - \nu). \tag{52}$$

However, all the remaining variables  $(z:=(q,\tilde{\theta})\in\mathbb{R}^{|\mathcal{N}|+|\mathcal{E}|}$  and  $\sigma:=(\alpha,\lambda,\eta,\nu)\in\mathbb{R}^{2|\mathcal{N}|+2|\mathcal{E}|+1})$  are updated using a saddle flow based on  $\bar{L}$  in (22) yet with  $p=p^{\ddagger}$ 

$$T^{z}\dot{z} = -\nabla_{z}\bar{L}(p, q, \tilde{\theta}, \alpha, \lambda, \eta, \nu)\Big|_{p=p^{\ddagger}}$$

$$T^{\sigma}\dot{\sigma} = \left[\nabla_{\sigma}\bar{L}(p, q, \tilde{\theta}, \alpha, \lambda, \eta, \nu)\Big|_{p=p^{\ddagger}}\right]_{\eta}^{+}$$
(53)

This variant of saddle flow dynamics (53) matches exactly the current closed-loop system (4), (44), and (49). However, it is not exactly a saddle flow because  $p^{\ddagger}$  is not the minimizer of p with respect to  $\bar{L}$  and, as a result, it does not correspond to any reduced planner's Lagrangian. Obviously, participants' bidding behavior is not aligned according to Definition 3.

# B. Market Modification

In this section, we propose a solution that modifies the market control laws (44) to accommodate such misaligned bidding behavior (49). To simplify the analysis and presentation, we still use the quadratic generation cost in (50). However, note that the idea of market modification is not limited to this particular case. We introduce an auxiliary primal variable  $\hat{q} \in \mathbb{R}^{|\mathcal{N}|}$  and reformulate the market problem with an extra regularization term in the objective function to minimize

$$U_m(q, \hat{q}; \alpha, \omega) := (\alpha + \omega)^T q + \frac{\rho}{2} \|q - \hat{q}\|^2$$
 (54a)

$$G_m(q, \hat{q}; \alpha, \omega) \le 0$$
 : (12c)-(12d) (54b)

where  $\rho > 0$  is a constant regularization coefficient. Due to the positive regularization, the minimum of (54) is lower bounded by that of (43) and the bound is tight only when  $q^* = \hat{q}^*$  holds. Therefore,  $(q^*, \hat{q}^* = q^*, \lambda^*, \eta^*)$  is optimal w.r.t. (54) if and only if  $(q^*, \lambda^*, \eta^*)$  is optimal w.r.t. (43). In this sense, we refer to  $\hat{q}$  as *virtual dispatch* since it is consistent with real dispatch q at optimality.

We still follow the general idea of gradient-based market control laws to define the Lagrangian  $L_m$  of (54):

$$L_m(q, \hat{q}, \lambda, \eta; \alpha, \omega) := (\alpha + \omega)^T q + \frac{\rho}{2} \|q - \hat{q}\|^2$$
$$-\lambda \cdot \mathbf{1}^T (q - d) + \eta^T \left(H^T (q - d) - F\right) \tag{55}$$

and select (25a) for  $(\hat{q}, \lambda, \eta)$  and (25b) for q, which yields the modified market dynamics

$$q \equiv \frac{1}{\rho} (\lambda \cdot \mathbf{1} - H\eta - \omega - \alpha) + \hat{q}$$
 (56a)

$$T^{\hat{q}}\dot{\hat{q}} = \lambda \cdot \mathbf{1} - H\eta - \omega - \alpha \tag{56b}$$

$$T^{\lambda}\dot{\lambda} = -\mathbf{1}^{T} \left( \frac{1}{\rho} (\lambda \cdot \mathbf{1} - H\eta - \omega - \alpha) + \hat{q} - d \right)$$
 (56c)

$$T^{\eta}\dot{\eta} = \left[H^T \left(\frac{1}{\rho}(\lambda \cdot \mathbf{1} - H\eta - \omega - \alpha) + \hat{q} - d\right) - F\right]_{\eta}^{+}.$$
(56a)

The virtual dispatch  $\hat{q}$  is internal to the market, whereas the real dispatch q is released to individual participants for implementation along with the clearing prices  $\pi = \lambda \cdot \mathbf{1} - H\eta - \omega$ .

## C. Equilibrium Analysis and Asymptotic Stability

In this section, we examine the interaction among the physical power network dynamics (4), the modified market control laws (56), and the rational bidding behavior (49) of individual participants. We will formally characterize the steady state and stability of this new closed-loop system.

We first define  $z := (\hat{q}, \tilde{\theta}) \in \mathbb{R}^{|\tilde{\mathcal{N}}| + |\mathcal{E}|}$  and  $\sigma := (\alpha, \lambda, \eta, \omega) \in \mathbb{R}^{2|\mathcal{N}| + 2|\mathcal{E}| + 1}$ , and note that q in (56a) is the reduced variable. We retain the sets of initial points and equilibrium points defined in (29) and (30), respectively. The corresponding equilibrium set is then explicitly characterized as follows (proof analogous to that of Theorem 2).

Theorem 4: For the grid–market–participant loop (4), (49), and (56), a point  $(z^*, \sigma^*) \in \mathbb{I}$  is an equilibrium if and only if  $(z^*, \sigma^*)$  corresponds to an optimal primal–dual solution to the planner's problem (12).

Having secured the desirable steady state, we next show that given the initial condition of  $\mathbb{I}$ , the grid–market–participant loop (4), (49), and (56) indeed converges to one equilibrium point in  $\mathbb{E}$  with proper choice of the coefficient  $\rho$ , as summarized below (proof in Appendix D).

Theorem 5: The equilibrium set  $\mathbb E$  is globally asymptotically stable on  $\mathbb I$ , given  $\rho \in (0,\inf_{j\in\mathcal N} 4c_j)$ . In particular, starting from any initial point in  $\mathbb I$ , a trajectory  $(z(t),\sigma(t))$  of the grid—market–participant loop (4), (49), and (56) remains bounded for  $t\geq 0$  and converges to  $(z^*,\sigma^*)$  with  $t\to\infty$ , where  $(z^*,\sigma^*)$  is one specific equilibrium point in  $\mathbb E$ .

Remark 2: Recall  $c_j > 0$ ,  $j \in \mathcal{N}$ , is the given quadratic coefficient in each generation cost function (50). Therefore, we can always pick a sufficiently small  $\rho$  that satisfies the condition such that the grid–market–participant loop (4), (49), and (56) asymptotically converges to a target equilibrium point.

Theorem 5 suggests that the proposed market modification with regularization (54) is able to accommodate the misalignment from the way each participant bids (49), such that the modified market dynamics and the misaligned individual bidding behavior can still function as a feedback controller on the power network dynamics to realize all the primary, secondary, and tertiary control with compatible participants' incentives. The required modification, however, highlights the necessity of *robust* market control laws that can better accommodate diverse participants' behavior and potential misalignment.

# D. Underlying Rationale: Implicit Regularization

In this section, we provide more intuitions about the modified market dynamics design (56). We first point out that the minimizer of the real dispatch q in (56a) is equivalent to the proximal operator (as a function of  $\hat{q}$ ) associated with the original  $L_m$  (in the variable q) in (42), and is commonly used in dealing with nondifferentiable optimization problems [28]. In light of the linear programming formulation of the original market problem (43), we can expect this proximal gradient-based market control laws (56) to secure convergence under milder conditions from an optimization perspective. We note, however, from a design perspective, the proposed market modification does not recover alignment to connect with standard saddle flows. Indeed, the current grid-market-participant loop (4), (49), and (56) still corresponds to the following improper form, yet with the Moreau–Yosida regularization on the original reduced Lagrangian L

$$T^{z}\dot{z} = -\nabla_{z} \left\{ \min_{q} \bar{L}(p, q, \tilde{\theta}, \alpha, \lambda, \eta, \nu) + \frac{\rho}{2} \|q - \hat{q}\|^{2} \right\} \Big|_{p=p^{\dagger}}$$

$$T^{\sigma}\dot{\sigma} = \left[ \nabla_{\sigma} \left\{ \min_{q} \bar{L}(p, q, \tilde{\theta}, \alpha, \lambda, \eta, \nu) + \frac{\rho}{2} \|q - \hat{q}\|^{2} \right\} \Big|_{p=p^{\dagger}} \right]_{\eta}^{+}$$
(57)

with  $z:=(\hat{q},\tilde{\theta})\in\mathbb{R}^{|\mathcal{N}|+|\mathcal{E}|}$  and  $\sigma:=(\alpha,\lambda,\eta,\nu)\in\mathbb{R}^{2|\mathcal{N}|+2|\mathcal{E}|+1}$  here. It is worth to highlight that the only difference between  $\bar{L}$  in (53) and the Moreau envelope of  $\bar{L}$  in (57)  $(\hat{q}$  in place of q) is an extra implicit regularization term

$$-\frac{1}{2\rho}\|\lambda \cdot \mathbf{1} - H\eta - \nu - \alpha\|^2. \tag{58}$$

Note that essentially the misaligned price bidding behavior (49) deviates from the aligned one (41) by using the clearing price information  $\pi = \lambda \cdot 1 - H\eta - \omega$  instead of the local bids  $\alpha$ . Thus, one can understand the role of the regularization term (58) as penalizing the mismatch between the clearing prices  $\pi$  and the local bids  $\alpha$ . The smaller the  $\rho$  is, the stronger this regularization impact will be and the closer the clearing prices  $\pi$  and the local bids  $\alpha$  will be tied to each other. Theorem 5 provides a threshold for  $\rho$  under which the two quantities are close enough such that the misalignment can be accommodated despite the use of the clearing price information.

Market Dynamics	Thermal Limits	Stability Guarantee	Alignment	Interoperability	Economic Rationality
Aligned Qty. Bidding	✓	✓	✓	✓	/
Aligned Price Bidding	✓	✓	✓	✓	<b> </b>
Misaligned Price Bidding	✓	✓	Х	✓	✓
Qty. Bidding Benchmark I	✓	Х	×	Х	Х
Qty. Bidding Benchmark II	✓ (only tree networks)	✓	✓	Х	Х
Price Bidding Benchmark	Х	✓	Х	Х	✓
Aligned Qty. Bidding  3 0  10 0 0 0 0 0 0 0 0 0 0 0 0 0 0 0 0 0	Aligned Price Bidding  0 50 100 150 200  Time t (s)	Misaligned Price Bidding  0 50 100 150 200  Time t (s)  (a) Frequency	0 50 100 150 200 Time t (s)		Price Bidding Benchmark  0 0 50 100 150 200  Time t (s)
Aligned Qty. Bidding $\begin{array}{cccc} & & & & & & & & \\ & & & & & & & \\ & & & & $	Aligned Price Bidding	Misaligned Price Bidding	Qty. Bidding Benchmark I	Qty. Bidding Benchmark I	Price Bidding Benchmark

TABLE I
PROPERTY COMPARISON ACROSS DIFFERENT MARKET DYNAMICS

Fig. 3. Comparison across different market dynamics in response to instant power imbalance: selected trajectories of frequency variables at generator buses 30–39 for (a) and line flow variables on lines 4, 19, and 26 for (b). (a) Frequency deviation. (b) Line flows (thermal limits indicated by dashed lines).

(b) Line flows (thermal limits indicated by dashed lines)

#### V. NUMERICAL RESULTS

We test the proposed aligned market dynamics based on quantity and price bidding, as well as the modified market dynamics for misaligned price bidding on the IEEE 39-bus system to illustrate their interplay with grid dynamics and respective participants' behavior. Despite basing our analysis on a linear approximation of the physical swing dynamics, we adopt a highfidelity model for the numerical tests, including nonlinear power flows, voltage dynamics, and first-order turbine dynamics. All of the ten generators, located at buses 30–39, are taken as market participants and can serve as prosumers by deviating from their nominal operating points. We randomly select three lines 4, 19, and 26, and endow them with relatively small transmission capacity  $\pm 3$  per unit (p.u.) such that the line thermal limits will be potentially binding. One p.u. (100 MW) of step load increase is imposed at bus 30 at time 0. The 200-s simulation runs of transient dynamics in response to this instant power imbalance for grid-market-participant loops will be presented, with selected trajectories of the frequency variables at generator buses 30–39 and the line flow variables on lines 4, 19, and 26.

Comparison Across Market Dynamics: We compare the three main market dynamics (37), (44), and (56) discussed in this article, along with three relevant benchmarks from the literature [20], [21], [22], [23]. In particular, we will refer to the benchmarks as follows: quantity bidding benchmark I—[20], quantity

bidding benchmark II—[21], and price bidding benchmark—[22] and [23]. Table I summarizes several key properties of market dynamics designs. It is apparent that the three market dynamics (37), (44), and (56) are designed in a more systematic manner that accounts for most, if not all, of these properties. As we can further observe from Fig. 3, all the three market dynamics (37), (44), and (56) are able to drive the respective systems to steady states within 200 s. At equilibrium, they all restore the frequency back to its nominal value, respect the line thermal limits, and achieve the optimal generation dispatch. However, the quantity bidding benchmark I fails to eliminate the frequency deviation. While the quantity bidding benchmark II and the price bidding benchmark restore the nominal frequency, congestion cannot be managed in both cases and there are steady-state line flows exceeding the thermal limits.

Performance of Market Modification: Fig. 4 shows a representative profile of frequency deviation at bus 37 with the modified market dynamics for misaligned price bidding, as we vary the regularization coefficient  $\rho$  subject to Theorem 5. The role of the regularization term (58) is enhanced with a smaller  $\rho$ , e.g., 0.1, which however amplifies oscillations in transient. On the

<sup>&</sup>lt;sup>8</sup>Alignment refers to the Lagrangian-based design of market control laws. Interoperability refers to the possibility of coexistence of dynamic gradient play (17a) and best response (17b) for individual bidding. Economic Rationality refers to the incentive-based bidding strategies (17).

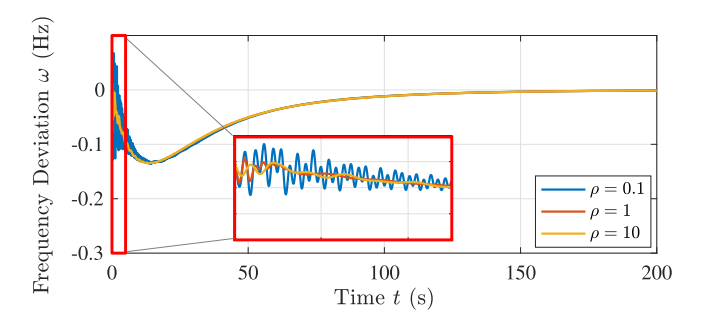


Fig. 4. Modified market dynamics for misaligned price bidding: Impact of  $\rho$  on frequency deviation at bus 37.

contrary, a larger  $\rho$ , e.g., 1 or 10, damps oscillations and leads to smoother convergence.

### VI. CONCLUSION

This article studies the interaction among grid dynamics, market dynamics, and bidding dynamics of individual market participants. We first develop a principled framework for the design and analysis of aligned market dynamics, conditioned on a family of alignment characterization for individual bidding behavior. The alignment connects the associated grid-marketparticipant loop to a saddle flow whose min-max saddle points, i.e., equilibrium points, optimally solve the target planner's problem to realize the primary, secondary, and tertiary frequency control with compatible participants' incentives. We show that the framework is general for the bidding mechanisms based on quantity and price, and, under mild conditions, the asymptotic convergence of the closed-loop system to an equilibrium can be guaranteed. Two specific examples of aligned market dynamics are demonstrated. We further study an exemplar of misaligned bidding behavior that can lead to system instability in the absence of the alignment property. A solution of modified market control laws is proposed to accommodate such misalignment, highlighting the necessity of market robustness against diverse individual bidding behavior. Numerical simulations on the IEEE 39-bus system validate our market dynamics designs in terms of global asymptotic stability and steady-state performance.

Limitations: There are several potential extensions that could help relax technical assumptions and make the results more general and robust. For example, general convex instead of quadratic costs may be necessary for the misaligned price bidding case. Further, local stability could be established in cases where convex costs do no hold. Practical factors, e.g., communication delay and state estimation error, are also important and will be left for future studies.

# APPENDIX A PROOF OF THEOREM 2

Define  $\phi := (p, q, \omega, \tilde{\theta}, \alpha, \lambda, \eta, \nu) \setminus (z, \sigma)$  to be the variables that are reduced and updated by taking their optimizers based on (17b), (20a), and (25b). Note that an optimal primal–dual solution to the planner's problem (12e) is characterized by the KKT conditions that include stationarity, primal feasibility, dual feasibility, and complementary slackness (assuming that certain regularity conditions hold).

*Necessary condition:* We first ignore the particular projection to guarantee  $\eta \geq 0$ . An equilibrium  $(z^*, \sigma^*)$  of the grid–market–participant loop (28) means

$$\nabla_z \hat{L}(z^*, \sigma^*) = 0 \tag{59a}$$

$$\nabla_{\sigma} \hat{L}(z^*, \sigma^*) = 0 \tag{59b}$$

with  $\hat{L}(z^*, \sigma^*) = L(z^*, \sigma^*, \phi(z^*, \sigma^*))$ , where  $\phi(z, \sigma)$  contains the corresponding optimizers of  $L(z, \sigma, \phi)$ , always satisfying

$$\nabla_{\phi} L(z^*, \sigma^*, \phi(z^*, \sigma^*)) = 0 \tag{59c}$$

due to the finiteness of  $\hat{L}$  by Assumption 1.9

Let  $\phi^* := \phi(z^*, \sigma^*)$  be the short hand. Note that (59a) and (59b) imply

$$\nabla_z \hat{L}(z^*, \sigma^*) = \left(\nabla_z L + \frac{\partial \phi}{\partial z}^T \nabla_\phi L\right) \bigg|_{(z^*, \sigma^*, \phi^*)} = 0 \quad (60a)$$

$$\nabla_{\sigma} \hat{L}(z^*, \sigma^*) = \left( \nabla_{\sigma} L + \frac{\partial \phi}{\partial \sigma}^T \nabla_{\phi} L \right) \bigg|_{(z^*, \sigma^*, \phi^*)} = 0 \quad (60b)$$

where  $\frac{\partial \phi}{\partial z}$  and  $\frac{\partial \phi}{\partial \sigma}$  constitute the Jacobian matrix of  $\phi(z,\sigma)$ . Equations (59c) and (60) jointly lead to

$$\nabla_z L(z^*, \sigma^*, \phi^*) = 0 \text{ and } \nabla_\sigma L(z^*, \sigma^*, \phi^*) = 0.$$
 (61)

Indeed, (59c) and (61) equate with all the stationarity conditions and equality feasibility conditions in the KKT conditions.

We next consider the effect of the projection for  $\eta \geq 0$ . If  $\eta$  is contained in  $\sigma$ , then we have

$$\left[\nabla_{\eta} \hat{L}(z^*, \sigma^*)\right]_{\eta}^{+} = \left[H^{T}(q^* - d) - F\right]_{\eta}^{+} = 0$$
 (62)

which suggests for any eth elements of these vectors either  $(H^T(q^*-d))_e = F_e$  with  $\eta_e^* \geq 0$  or  $(H^T(q^*-d))_e < F_e$  with  $\eta_e^* = 0$ . In either case, the inequality feasibility conditions [(12d) and  $\eta \geq 0$ ] and the complementary slackness condition are simultaneously guaranteed.

If  $\eta$  is contained in  $\phi$ , then it follows from (25b) and Assumption 1 that:

$$\nabla_n L(z^*, \sigma^*, \phi^*) \le 0$$
 and  $\operatorname{diag}(\eta^*) \nabla_n L(z^*, \sigma^*, \phi^*) = 0$  (63)

should hold to guarantee the finiteness of  $\hat{L}$  in the presence of  $\eta \geq 0$ . Therefore, the inequality feasibility conditions and the complementary slackness condition are also met.

All in all, the KKT conditions are satisfied and  $(z^*, \sigma^*, \phi^*)$  is an optimal solution to the planner's problem (12).

Sufficient condition: Given an optimal solution  $(z^*, \sigma^*, \phi^*)$  to the planner's problem (12) that satisfies the KKT conditions, if  $\eta$  is contained in  $\sigma$ , then all the stationarity conditions and equality feasibility conditions basically equate with (59c) and (61), and thus (59a) and (59b), for all the variables except  $\eta$ . Further, the inequality feasibility condition (12d) suggests  $\nabla_{\eta} \hat{L}(z^*, \sigma^*) = 0$  immediately if it attains equality; otherwise,

 $<sup>^9</sup>$ As discussed in Remark 1, the potential regularization technique guarantees the uniqueness and Lipschitz continuity of  $\phi(z,\sigma)$ , and thus also the existence of its Jacobian matrix in our problem.

the complementary slackness condition mandates  $\eta^*=0$ , which projects the negative  $\nabla_{\eta}\hat{L}(z^*,\sigma^*)$  to zero through the projection  $[\cdot]_{\eta}^+$ . Therefore,  $(z^*,\sigma^*)$  is an equilibrium point of (28).

If  $\eta$  is contained in  $\phi$ , indeed the optimality condition of (25b) suggests that

$$\operatorname{diag}(\eta)\nabla_{\eta}L(z,\sigma,\phi) = \operatorname{diag}(\eta)\left(H^{T}(q-d) - F\right) = 0 \quad (64)$$

should always hold, by Assumption 1. In this case,  $\hat{L}$  is independent of  $\eta$ . Then, all the stationarity conditions and equality feasibility conditions in the KKT conditions suffice to show (59a) and (59b) and validate that  $(z^*, \sigma^*)$  is still an equilibrium point of (28).

# APPENDIX B PROOF OF THEOREM 3

We explicitly demonstrate the asymptotic convergence of the grid–market–participant loop (28). Let the largest invariant set between the ON–OFF switches of the projection  $[\cdot]_{\eta}^{+}$  be

$$\mathbb{S} := \left\{ (z, \sigma) \mid \dot{V}(z(t), \sigma(t)) \equiv 0, \ t \in \mathbb{R}_{\geq 0} \backslash \mathbb{T} \right\}$$
 (65)

where  $V(z,\sigma)$  is a real-valued Lyapunov function and  $\mathbb T$  consists of all the time epochs when the projection switches between ON and OFF. The whole proof boils down to the following three steps.

- 1) Step 1: Each trajectory  $(z(t), \sigma(t))$  converges to the largest invariant set  $\mathbb{S}$ .
- 2) Step 2: Any trajectory  $(z(t), \sigma(t))$  in the set  $\mathbb{S}$  is an equilibrium of the closed-loop system (28), i.e.,  $\mathbb{S} \subset \mathbb{E}$ .
- 3) Step 3: Each trajectory  $(z(t), \sigma(t))$  literally converges to a single equilibrium point of the closed-loop system (28).

We next prove each individual step.

Step 1: The grid–market–participant loop (28) is essentially implementing a (projected) saddle flow on  $\hat{L}(z,\sigma)$ , and each equilibrium point  $(z^*,\sigma^*)$  is therefore a min–max saddle point of  $\hat{L}(z,\sigma)$  (within a specified domain). Consider the following quadratic Lyapunov function for  $V(\cdot)$ :

$$V(z,\sigma) := \frac{1}{2} \begin{bmatrix} z - z^* \\ \sigma - \sigma^* \end{bmatrix}^T \begin{bmatrix} T^z \\ T^\sigma \end{bmatrix} \begin{bmatrix} z - z^* \\ \sigma - \sigma^* \end{bmatrix}$$
(66)

where  $(z^*, \sigma^*)$  is one arbitrary equilibrium point of the closed-loop system (28). The Lie derivative of  $V(z, \sigma)$  along the trajectory of  $(z(t), \sigma(t))$  is given by

$$\dot{V}(z,\sigma)$$

$$= (z - z^*)^T T^z \dot{z} + (\sigma - \sigma^*)^T T^\sigma \dot{\sigma}$$
(67a)

$$= -(z - z^*)^T \nabla_z \hat{L}(z, \sigma) + (\sigma - \sigma^*)^T \left[ \nabla_\sigma \hat{L}(z, \sigma) \right]_n^+$$
 (67b)

$$\leq -(z-z^*)^T \nabla_z \hat{L}(z,\sigma) + (\sigma-\sigma^*)^T \nabla_\sigma \hat{L}(z,\sigma)$$
 (67c)

$$\leq \hat{L}(z^*,\sigma) - \hat{L}(z,\sigma) + \hat{L}(z,\sigma) - \hat{L}(z,\sigma^*) \tag{67d}$$

$$= \underbrace{\hat{L}(z^*, \sigma) - \hat{L}(z^*, \sigma^*)}_{<0} + \underbrace{\hat{L}(z^*, \sigma^*) - \hat{L}(z, \sigma^*)}_{<0}. \tag{67e}$$

Equation (67b) applies (28). Equation (67c) uses the non-expansive property of the projection  $[\cdot]^+_{\eta}$  demonstrated in (2). Equation (67d) results from the convexity (respectively, concavity) of  $\hat{L}(z,\sigma)$  in z (respectively,  $\sigma$ ). Equation (67e) finally follows from the saddle property of the equilibrium point  $(z^*,\sigma^*)$ .

Since  $V(z,\sigma)$  is radially unbounded,  $V(z,\sigma) \leq 0$  indicates that all the trajectories  $(z(t),\sigma(t))$  remain bounded. It then follows from the invariance principle for Caratheodory systems [30] that  $(z(t),\sigma(t))$  converges to the largest invariant set  $\mathbb S$ .

Step 2: For any trajectory  $(z(t), \sigma(t)) \in \mathbb{S}$ ,  $\dot{V}(z, \sigma) \equiv 0$  enforces (67e) to be zero with

$$\hat{L}(z(t), \sigma^*) \equiv \hat{L}(z^*, \sigma^*)$$
 and  $\hat{L}(z^*, \sigma(t)) \equiv \hat{L}(z^*, \sigma^*)$ . (68)

By Assumption 2, we have  $\dot{z} \equiv 0$  and  $\dot{\sigma} \equiv 0$  for any trajectory  $(z(t), \sigma(t))$  in the largest invariant set  $\mathbb{S}$ , which is therefore an equilibrium of the closed-loop system (28), i.e.,  $\mathbb{S} \subset \mathbb{E}$ .

Step 3: We now show any trajectory  $(z(t),\sigma(t))$  indeed converges to one single equilibrium. First of all, along any trajectory  $(z(t),\sigma(t)),\ V(z,\sigma)$  is nonincreasing in t. Since  $V(z,\sigma)$  is lower bounded given its quadratic form, there exists an infinite sequence of time epochs  $\{t_k,k=1,2,\dots\}$  such that with  $k\to\infty$ , we have  $\dot{V}(z(t_k),\sigma(t_k))\to 0$ , i.e.,  $(z(t_k),\sigma(t_k))\to (\hat{z}^*,\hat{\sigma}^*)\in\mathbb{S}\subset\mathbb{E}$ . We use this specific  $(\hat{z}^*,\hat{\sigma}^*)$  as the equilibrium point in the definition of  $V(z,\sigma)$ , which implies  $V(z(t),\sigma(t))\to V(\hat{z}^*,\hat{\sigma}^*)=0$ . Due to the continuity of  $V(z,\sigma),\ (z(t),\sigma(t))\to (\hat{z}^*,\hat{\sigma}^*)$  is enforced, which therefore suggests that  $(z(t),\sigma(t))$  indeed converges to one single equilibrium point in  $\mathbb{S}\subset\mathbb{E}$ .

# APPENDIX C PROOF OF PROPOSITION 1

Given  $\hat{L}$  in (38) and an arbitrary trajectory  $(z(t), \sigma(t))$  of the grid–market–participant loop (28) that satisfies

$$\hat{L}(z(t), \sigma^*) \equiv \hat{L}(z^*, \sigma^*) \tag{69}$$

and

$$\hat{L}(z^*, \sigma(t)) \equiv \hat{L}(z^*, \sigma^*) \tag{70}$$

differentiating (69) with respect to time yields

$$0 \equiv \left(\nabla_z \hat{L}(z(t), \sigma^*)\right)^T \dot{z}$$

$$\equiv -\left(\nabla_z \hat{L}(z(t), \sigma^*)\right)^T T^{z-1} \nabla_z \hat{L}(z(t), \sigma^*) \tag{71}$$

which indicates  $\nabla_z \hat{L}(z(t), \sigma^*) \equiv 0$  due to  $T^{z-1} \succ 0$ . Given  $\sigma^*$ , the fact of  $\nabla_p \hat{L}(z(t), \sigma^*) \equiv 0$  enforces  $p(t) \equiv p^*$ , due to the monotonicity of  $\nabla J(\cdot)$ .

Similarly, differentiating (70) with respect to time gives

$$0 \equiv \left(\nabla_{\sigma} \hat{L}(z^*, \sigma(t))\right)^T \dot{\sigma}$$

$$\equiv \left(\nabla_{\sigma} \hat{L}(z^*, \sigma(t))\right)^T T^{\sigma - 1} \left[\nabla_{\sigma} \hat{L}(z^*, \sigma(t))\right]_n^+ \tag{72}$$

which still enforces  $\nabla_{\nu}\hat{L}(z^*,\sigma(t))\equiv 0, \ \nabla_{\lambda}\hat{L}(z^*,\sigma(t))\equiv 0,$  and meanwhile

$$\left(\nabla_{\eta}\hat{L}(z^*, \sigma(t))\right)^T T^{\eta - 1} \left[\nabla_{\eta}\hat{L}(z^*, \sigma(t))\right]_{\eta}^+ \equiv 0 \tag{73}$$

due to  $T^{\sigma^{-1}} \succ 0$ . Given  $p(t) \equiv p^*$ , the fact of  $\nabla_\lambda \hat{L}(z^*, \sigma(t)) \equiv 0$  implies  $\dot{\lambda} \equiv 0$ . Meanwhile, in terms of (73), the inner term  $H^T(p^*-d) - F$  of the projection  $[\cdot]^+_\eta$  is a constant vector. Consider an arbitrary eth element of the vector that falls into three cases: (a)  $(H^T(p^*-d)-F)_e > 0$ , (b)  $(H^T(p^*-d)-F)_e = 0$ , and (c)  $(H^T(p^*-d)-F)_e < 0$ . In case (a),  $\dot{\eta}_e > 0$  drives  $\eta_e(t)$  to infinity, which cannot happen since all the trajectories in the largest invariant set  $\mathbb S$  are bounded. Case (b) immediately implies  $\dot{\eta}_e \equiv 0$ . In case (c), since  $T^{\eta-1} \succ 0$  is diagonal,  $(\nabla_\eta \hat{L}(z^*,\sigma(t)))_e < 0$  enforces  $[(\nabla_\eta \hat{L}(z^*,\sigma(t)))_e]^+_{\eta_e} \equiv 0$ , i.e.,  $\dot{\eta}_e \equiv 0$ , in order for (73) to hold. As a result,  $\dot{\eta} \equiv 0$  is guaranteed. On top of  $\dot{\lambda} \equiv 0$  and  $\dot{\eta} \equiv 0$ ,  $T^p\dot{p} = \lambda(t) \cdot 1 - H\eta(t) - \nu(t) - \nabla_p J(p^*) \equiv 0$  enforces  $\dot{\nu} \equiv 0$ , or  $\nu(t) \equiv \bar{\nu}$ , where  $\bar{\nu}$  is constant. The fact of  $\nabla_\nu \hat{L}(z^*,\sigma(t)) \equiv 0$  suggests

$$p^* - d - D\bar{\nu} - CB\tilde{\theta}^* \equiv 0. \tag{74}$$

Due to  $p^*-d-D\nu^*-CB\tilde{\theta}^*=0$  from (12b) and (12e),  $\nu(t)\equiv\bar{\nu}=\nu^*=0$  follows immediately due to  $D\succ 0$ , which further implies  $\dot{\tilde{\theta}}\equiv 0$ . This completes the proof of  $\dot{z}\equiv 0$  and  $\dot{\sigma}=0$ 

# APPENDIX D PROOF OF THEOREM 5

Recall the quadratic form of generation cost functions (50), parameterized by  $c:=(c_j,j\in\mathcal{N})$  and  $\bar{c}:=(\bar{c}_j,j\in\mathcal{N})$ . We further define  $c^{-1}:=(c_j^{-1},j\in\mathcal{N})$ . Therefore, (49) can be more explicitly expressed as

$$T^{\alpha}\dot{\alpha} = \frac{1}{\rho}(\lambda \cdot \mathbf{1} - H\eta - \omega - \alpha) + \hat{q} - \operatorname{diag}(c^{-1})(\lambda \cdot \mathbf{1} - H\eta - \omega - \bar{c}). \tag{75}$$

With the closed-loop system (4), (49), and (56) defined on  $z=(\hat{q},\tilde{\theta})$  and  $\sigma=(\lambda,\omega,\alpha,\eta),^{10}$  we can define a square matrix  $W\in\mathbb{R}^{(3|\mathcal{N}|+3|\mathcal{E}|+1)\times(3|\mathcal{N}|+3|\mathcal{E}|+1)}$  to summarize the right-hand side linear dependence of the differential equations (4), (49), and (56) on  $(z,\sigma)$  such that we attain a more compact form

$$\begin{bmatrix} T^z \\ T^\sigma \end{bmatrix} \begin{bmatrix} \dot{z} \\ \dot{\sigma} \end{bmatrix} = \begin{bmatrix} W \begin{bmatrix} z \\ \sigma \end{bmatrix} + \beta \end{bmatrix}_{\eta}^{+}$$
 (76)

with a constant input  $\beta \in \mathbb{R}^{3|\mathcal{N}|+3|\mathcal{E}|+1}$  given by

$$\beta := \begin{bmatrix} 0 & 0 & \mathbf{1}^T d & -d^T & \bar{c}^T \mathrm{diag}(c^{-1}) & -d^T H - F^T \end{bmatrix}^T. \tag{77}$$

We focus on the trajectories  $(z(t), \sigma(t))$  that start with initial points in  $\mathbb{I}$ . Note that we still have the equilibrium set and the largest invariant set denoted as  $\mathbb{E}$  and  $\mathbb{S}$ , respectively, from (30) and (65). Given the condition  $\rho \in (0, \inf_{i \in \mathcal{N}} 4c_i)$ , the whole

 $^{10}$ Without loss of generality, we rearrange the variables in  $\sigma$  for ease of analysis and presentation.

proof still follows the same three steps in the proof of Theorem 3 in Appendix B. We now show each individual step.

Step 1: We still adopt the standard quadratic Lyapunov function (66), but now  $(z^*, \sigma^*)$  is one arbitrary equilibrium point of the closed-loop system (4), (49), and (56). We can acquire the Lie derivative of  $V(z, \sigma)$  along the trajectory of  $(z(t), \sigma(t))$  as

$$\dot{V}(z,\sigma) = \begin{bmatrix} z - z^* \\ \sigma - \sigma^* \end{bmatrix}^T \begin{bmatrix} T^z \dot{z} \\ T^\sigma \dot{\sigma} \end{bmatrix}$$
 (78a)

$$= \begin{bmatrix} z - z^* \\ \sigma - \sigma^* \end{bmatrix}^T \left[ W \begin{bmatrix} z \\ \sigma \end{bmatrix} + \beta \right]_{\eta}^+ \le \begin{bmatrix} z - z^* \\ \sigma - \sigma^* \end{bmatrix}^T \left( W \begin{bmatrix} z \\ \sigma \end{bmatrix} + \beta \right)$$
(78b)

$$= \begin{bmatrix} z - z^* \\ \sigma - \sigma^* \end{bmatrix}^T W \begin{bmatrix} z - z^* \\ \sigma - \sigma^* \end{bmatrix} - (\eta - \eta^*)^T \psi^*$$
 (78c)

$$\leq \begin{bmatrix} z - z^* \\ \sigma - \sigma^* \end{bmatrix}^T W \begin{bmatrix} z - z^* \\ \sigma - \sigma^* \end{bmatrix} = -(\sigma - \sigma^*)^T W_{\sigma}(\sigma - \sigma^*) \tag{78d}$$

where  $\psi^* \in \mathbb{R}^{2|\mathcal{E}|}_{\geq 0}$  denotes a complementary vector variable, and  $W_{\sigma} \in \mathbb{R}^{(2|\mathcal{N}|+2|\mathcal{E}|+1)\times(2|\mathcal{N}|+2|\mathcal{E}|+1)}$ , with its explicit expression in (80) shown at the bottom of this page, is a symmetric matrix rearranged from the submatrix of -W that contains all the rows and columns with regard to  $\sigma$ . Note that (78c) follows from the equilibrium condition:

$$W\begin{bmatrix} z^* \\ \sigma^* \end{bmatrix} + \beta + \begin{bmatrix} 0^{3|\mathcal{N}| + |\mathcal{E}| + 1} \\ \psi^* \end{bmatrix} = 0 \tag{79}$$

along with the complementarity condition  $0 \le \eta^* \perp \psi^* \ge 0$ . The inequality in (78d) results from the fact  $(\eta - \eta^*)^T \psi^* = \eta^T \psi^* - \eta^{*T} \psi^* = \eta^T \psi^* \ge 0$ , and the equality in (78d) is attained with all the terms regarding  $z-z^*$  canceled out due to the specific structure of W. We show next the positive semidefiniteness of  $W_\sigma$ . Let  $R:=I-\frac{\rho}{2}\cdot \mathrm{diag}(c^{-1})$  be a diagonal matrix and  $W_\sigma$  can be rewritten as

$$W_{\sigma} = \rho^{-1} Q^{T} \begin{bmatrix} I & -I & -R & -I \\ -I & I + \rho D & R & I \\ -R & R & I & R \\ -I & I & R & I \end{bmatrix} Q$$
(81)

with  $Q:=\operatorname{blockdiag}(\mathbf{1},I,I,H)\in\mathbb{R}^{4|\mathcal{N}|\times(2|\mathcal{N}|+2|\mathcal{E}|+1)}$ . The inner matrix  $W^{\mathrm{in}}_{\sigma}\in\mathbb{R}^{4|\mathcal{N}|\times4|\mathcal{N}|}$  of (81) can be further block diagonalized by the following bijective linear transformation

$$W_{\sigma} := \begin{bmatrix} |\mathcal{N}|\rho^{-1} & -\rho^{-1} \cdot \mathbf{1}^{T} & \frac{1}{2} \cdot c^{-1}^{T} - \rho^{-1} \cdot \mathbf{1}^{T} & -\rho^{-1} \cdot \mathbf{1}^{T} H \\ -\rho^{-1} \cdot \mathbf{1} & \rho^{-1} \cdot I + D & \rho^{-1} \cdot I - \frac{1}{2} \cdot \operatorname{diag}(c^{-1}) & \rho^{-1} \cdot H \\ \frac{1}{2} \cdot c^{-1} - \rho^{-1} \cdot \mathbf{1} & \rho^{-1} \cdot I - \frac{1}{2} \cdot \operatorname{diag}(c^{-1}) & \rho^{-1} \cdot I & (\rho^{-1} \cdot I - \frac{1}{2} \cdot \operatorname{diag}(c^{-1})) H \\ -\rho^{-1} \cdot H^{T} \mathbf{1} & \rho^{-1} \cdot H^{T} & H^{T} \left(\rho^{-1} \cdot I - \frac{1}{2} \cdot \operatorname{diag}(c^{-1})\right) & \rho^{-1} \cdot H^{T} H \end{bmatrix}. \tag{80}$$

 $P \in \mathbb{R}^{4|\mathcal{N}|\times 4|\mathcal{N}|}$ :  $W_{\sigma} = \rho^{-1}Q^T P^T \hat{W}_{\sigma} PQ$ , with

$$\hat{W}_{\sigma} := \begin{bmatrix} I & 0 & 0 & 0 \\ 0 & \rho D & 0 & 0 \\ 0 & 0 & I - R^2 & 0 \\ 0 & 0 & 0 & 0 \end{bmatrix}, \quad P := \begin{bmatrix} I & I & R & I \\ 0 & I & 0 & 0 \\ 0 & 0 & I & 0 \\ 0 & 0 & 0 & I \end{bmatrix}^{-1}.$$
(82)

Note that  $I-R^2$  is still diagonal and it is easy to verify that any arbitrary  $\rho \in (0,\inf_{j\in\mathcal{N}}4c_j)$  guarantees its positive definiteness.  $W_\sigma\succeq 0$  then follows from  $I\succ 0,\ \rho D\succ 0$ , and  $I-R^2\succ 0$ .

Therefore, following (78d), we arrive at:

$$\dot{V}(z,\sigma) \le -(\sigma - \sigma^*)^T W_{\sigma}(\sigma - \sigma^*) \le 0. \tag{83}$$

Since  $V(z,\sigma)$  is radially unbounded,  $\dot{V}(z,\sigma) \leq 0$  indicates that all the trajectories  $(z(t),\sigma(t))$  remain bounded. It then follows from the invariance principle for Caratheodory systems that  $(z(t),\sigma(t))$  converges to the largest invariant set  $\mathbb S$ .

Step 2: For an arbitrary trajectory  $(z(t), \sigma(t)) \in \mathbb{S}$ ,  $V(z, \sigma) \equiv 0$  basically enforces  $(\sigma - \sigma^*)^T W_{\sigma}(\sigma - \sigma^*) \equiv 0$ . In light of the structure of  $W_{\sigma}$  in (81), its semidefiniteness results from the nontrivial null space of  $W_{\sigma}^{\text{in}}$  and Q. As a result, we can characterize the largest invariant set  $\mathbb{S}$  as the union of the following three sets:

$$\mathbb{S}_{1} := \{(z, \sigma) \mid \sigma(t) \equiv \sigma^{*}\}$$

$$\mathbb{S}_{2} := \{(z, \sigma) \mid H(\eta(t) - \eta^{*}) \equiv 0, \lambda(t) \equiv \lambda^{*}, \omega(t) \equiv \omega^{*},$$

$$\times \alpha(t) \equiv \alpha^{*}\}$$

$$\mathbb{S}_{3} := \{(z, \sigma) \mid (\lambda(t) - \lambda^{*}) \cdot \mathbf{1} \equiv H(\eta(t) - \eta^{*}), \omega(t) \equiv \omega^{*},$$

$$\times \alpha(t) \equiv \alpha^{*}\}.$$

We next show  $\mathbb{S}_2 \equiv \mathbb{S}_3$  by first claiming  $\mathbf{1}^T H = 0$ . Recall  $H = [(BC^T L^\dagger)^T, -(BC^T L^\dagger)^T]$  and  $L = CBC^T$ . By definition of the Moore–Penrose inverse, it is straightforward to have  $L^\dagger \mathbf{1} = 0$ , which immediately suggests  $\mathbf{1}^T H = 0$ .

In 
$$S_3$$
,  $(\lambda(t) - \lambda^*) \cdot \mathbf{1} \equiv H(\eta(t) - \eta^*)$  leads to
$$\underbrace{\mathbf{1}^T \cdot (\lambda(t) - \lambda^*) \cdot \mathbf{1}}_{-|\Lambda(t)(t)|} \equiv \underbrace{\mathbf{1}^T H(\eta(t) - \eta^*)}_{-0}$$
(84)

which enforces  $\lambda(t) \equiv \lambda^*$  and  $H(\eta(t) - \eta^*) \equiv 0$ , i.e.,  $\mathbb{S}_3 \subset \mathbb{S}_2$ . Obviously, by definition, we have  $\mathbb{S}_2 \subset \mathbb{S}_3$ . Therefore,  $\mathbb{S}_2$  and  $\mathbb{S}_3$  are equivalent.

Note that in any of the three sets, we have  $\lambda(t) \equiv \lambda^*, \, \omega(t) \equiv \omega^*, \, \alpha(t) \equiv \alpha^*, \, \text{and} \, H\eta(t) \equiv H\eta^*, \, \text{which suffice to guarantee}$   $\dot{\hat{q}} \equiv 0$  and  $\dot{\tilde{\theta}} \equiv 0$  immediately, or  $\dot{z} \equiv 0$ ; recall (4a) and (56b). Then, it suggests that the inner term of the projection  $[\cdot]^+_{\eta}$  in (56d) is a constant vector. For its eth entry, it could be (a) positive, (b) zero, and (c) negative. In case (a),  $\dot{\eta}_e > 0$  drives  $\eta_e(t)$  to infinity, which contradicts the fact that all the trajectories in the largest invariant set  $\mathbb S$  are bounded. Case (b) directly implies  $\dot{\eta}_e \equiv 0$ . In case (c),  $\eta_e(t)$  will be driven to stay at 0 that also suggests  $\dot{\eta}_e \equiv 0$ . As a result,  $\dot{\eta} \equiv 0$  holds.  $^{11}$  So far,  $\dot{\sigma} \equiv 0$  has also been

guaranteed. Therefore, any trajectory  $(z(t), \sigma(t))$  in the largest invariant set  $\mathbb S$  is an equilibrium of the closed-loop system (4), (49), and (56), i.e.,  $\mathbb S \subset \mathbb E$ .

Step 3: We now prove any trajectory  $(z(t), \sigma(t))$  indeed converges to one single equilibrium for completeness, despite similar procedures to Step 3 in the proof of Theorem 3. We observe that along any trajectory  $(z(t), \sigma(t)), V(z, \sigma)$  is nonincreasing in t. Since  $V(z, \sigma)$  is lower bounded given its quadratic form, there exists an infinite sequence of time epochs  $\{t_k, k = 1, 2, \dots\}$  such that with  $k \to \infty$ , we have  $\dot{V}(z(t_k), \sigma(t_k)) \to 0$ , i.e.,  $(z(t_k), \sigma(t_k)) \to (\hat{z}^*, \hat{\sigma}^*) \in \mathbb{S} \subset \mathbb{E}$ . We use this specific  $(\hat{z}^*, \hat{\sigma}^*)$  as the equilibrium point in the definition of  $V(z, \sigma)$ , which implies  $V(z(t), \sigma(t)) \to V(\hat{z}^*, \hat{\sigma}^*) = 0$ . Due to the continuity of  $V(z, \sigma), (z(t), \sigma(t)) \to (\hat{z}^*, \hat{\sigma}^*)$  is enforced, which suggests that  $(z(t), \sigma(t))$  literally converges to one single equilibrium point in  $\mathbb{S} \subset \mathbb{E}$ .

#### **REFERENCES**

- [1] P. You, J. Z. F. Pang, and E. Yeung, "Stabilization of power networks via market dynamics," in *Proc. ACM Int. Conf. Future Energy Syst. (e-Energy)*, 2018, pp. 139–145.
- [2] D. S. Kirschen and G. Strbac, Fundamentals of Power System Economics. Hoboken, NJ, USA: Wiley, 2018.
- [3] F. L. Alvarado, J. Meng, C. L. DeMarco, and W. S. Mota, "Stability analysis of interconnected power systems coupled with market dynamics," *IEEE Trans. Power Syst.*, vol. 16, no. 4, pp. 695–701, Nov. 2001.
- [4] J. Machowski, J. Bialek, J. R. Bumby, and J. Bumby, Power System Dynamics and Stability. Hoboken, NJ, USA: Wiley, 1997.
- [5] A. J. Wood, B. F. Wollenberg, and G. B. Sheblé, *Power Generation, Operation, and Control.* Hoboken, NJ, USA: Wiley, 2013.
- [6] C. Zhao, E. Mallada, S. Low, and J. Bialek, "A unified framework for frequency control and congestion management," in *Proc. IEEE Power* Syst. Computation Conf., 2016, pp. 1–7.
- [7] N. Li, C. Zhao, and L. Chen, "Connecting automatic generation control and economic dispatch from an optimization view," *IEEE Trans. Control Netw. Syst.*, vol. 3, no. 3, pp. 254–264, Sep. 2016.
- [8] E. Mallada, C. Zhao, and S. Low, "Optimal load-side control for frequency regulation in smart grids," *IEEE Trans. Autom. Control*, vol. 62, no. 12, pp. 6294–6309, Dec. 2017.
- [9] Z. Wang, F. Liu, S. H. Low, C. Zhao, and S. Mei, "Distributed frequency control with operational constraints, Part I: Per-node power balance," *IEEE Trans. Smart Grid*, vol. 10, no. 1, pp. 40–52, Jan. 2019.
- [10] Z. Wang, F. Liu, S. H. Low, C. Zhao, and S. Mei, "Distributed frequency control with operational constraints, Part II: Network power balance," *IEEE Trans. Smart Grid*, vol. 10, no. 1, pp. 53–64, Jan. 2019.
- [11] E. Weitenberg, Y. Jiang, C. Zhao, E. Mallada, C. De Persis, and F. Dörfler, "Robust decentralized secondary frequency control in power systems: Merits and tradeoffs," *IEEE Trans. Autom. Control*, vol. 64, no. 10, pp. 3967–3982, Oct. 2019.
- [12] J. Z. Pang, L. Guo, and S. H. Low, "Optimal load control for frequency regulation under limited control coverage," in *Proc. IREP Symp.*, 2017, pp. 1–7.
- [13] F. Dorfler, J. W. Simpson-Porco, and F. Bullo, "Breaking the hierarchy: Distributed control and economic optimality in microgrids," *IEEE Trans. Control Netw. Syst.*, vol. 3, no. 3, pp. 241–253, Sep. 2016.
- [14] D. Cai, E. Mallada, and A. Wierman, "Distributed optimization decomposition for joint economic dispatch and frequency regulation," *IEEE Trans. Power Syst.*, vol. 32, no. 6, pp. 4370–4385, Nov. 2017.
- [15] Y. G. Jin, S. Y. Lee, S. W. Kim, and Y. T. Yoon, "Designing rule for price-based operation with reliability enhancement by reducing the frequency deviation," *IEEE Trans. Power Syst.*, vol. 28, no. 4, pp. 4365–4372, Nov. 2013.
- [16] D. Watts and F. L. Alvarado, "The influence of futures markets on real time price stabilization in electricity markets," in *Proc. IEEE Annu. Hawaii Int. Conf. Syst. Sci.*, 2004, pp. 1–7.
- [17] W. S. Mota and F. L. Alvarado, "Dynamic coupling between power markets and power systems with congestion constraints," in *Proc. IEEE Porto PowerTech*, 2001, pp. 1–6.
- [18] A. Kiani and A. Annaswamy, "The effect of a smart meter on congestion and stability in a power market," in *Proc. IEEE Conf. Decis. Control*, 2010, pp. 194–199.

<sup>&</sup>lt;sup>11</sup>There might exist a trivial degenerate subspace in case (c), where  $H(\eta(t)-\eta^*)\equiv 0$  holds with  $\dot{\eta}\not\equiv 0$ . However, in this subspace, if any, the system is still in transient and will eventually converge to  $\eta(t)\equiv\eta^*$ . Therefore, we exclude it from the characterization of § for conciseness.

- [19] Y. Liang, F. Liu, and S. Mei, "Stability analysis of the hybrid dynamics coupling power systems with power markets," in *Proc. IEEE Power Energy* Soc. Gen. Meeting, 2015, pp. 1–5.
- [20] A. Jokić, M. Lazar, and P. P. van den Bosch, "Real-time control of power systems using nodal prices," *Int. J. Elect. Power Energy Syst.*, vol. 31, no. 9, pp. 522–530, 2009.
- [21] T. Stegink, C. De Persis, and A. van der Schaft, "A unifying energy-based approach to stability of power grids with market dynamics," *IEEE Trans. Autom. Control*, vol. 62, no. 6, pp. 2612–2622, Jun. 2017.
- [22] A. Cherukuri, T. Stegink, C. De Persis, A. van der Schaft, and J. Cortés, "Frequency-driven market mechanisms for optimal dispatch in power networks," *Automatica*, vol. 133, 2021, Art. no. 109861.
- [23] T. Stegink, A. Cherukuri, C. De Persis, A. Van der Schaft, and J. Cortés, "Hybrid interconnection of iterative bidding and power network dynamics for frequency regulation and optimal dispatch," *IEEE Trans. Control Netw.* Syst., vol. 6, no. 2, pp. 572–585, Jun. 2019.
- [24] P. Kundur, N. J. Balu, and M. G. Lauby, Power System Stability and Control. New York, NY, USA: McGraw-Hill, 1994.
- [25] J. S. Shamma and G. Arslan, "Dynamic fictitious play, dynamic gradient play, and distributed convergence to Nash equilibria," *IEEE Trans. Autom. Control*, vol. 50, no. 3, pp. 312–327, Mar. 2005.
- [26] D. Goldsztajn, F. Paganini, and A. Ferragut, "Proximal optimization for resource allocation in distributed computing systems with data locality," in *Proc. IEEE Annu. Allerton Conf. Commun., Control, Comput.*, 2019, pp. 773–780.
- [27] P. You and E. Mallada, "Saddle flow dynamics: Observable certificates and separable regularization," in *Proc. IEEE Amer. Control Conf.*, 2021, pp. 4817–4823.
- [28] N. K. Dhingra, S. Z. Khong, and M. R. Jovanović, "The proximal augmented Lagrangian method for nonsmooth composite optimization," *IEEE Trans. Autom. Control*, vol. 64, no. 7, pp. 2861–2868, Jul. 2019.
- [29] A. Cherukuri, E. Mallada, S. Low, and J. Cortés, "The role of convexity in saddle-point dynamics: Lyapunov function and robustness," *IEEE Trans. Autom. Control*, vol. 63, no. 8, pp. 2449–2464, Aug. 2018.
   [30] A. Bacciotti and F. Ceragioli, "Nonpathological Lyapunov functions
- [30] A. Bacciotti and F. Ceragioli, "Nonpathological Lyapunov functions and discontinuous Carathéodory systems," *Automatica*, vol. 42, no. 3, pp. 453–458, 2006.



**Pengcheng You** (Member, IEEE) received the B.S. and Ph.D. degrees in control from Zhejiang University, Hangzhou, China, in 2013 and 2018, respectively.

During the graduate studies, he was a Visiting Student with Caltech and a Research Intern with PNNL. He is currently an Assistant Professor with the Department of Industrial Engineering and Management, College of Engineering, Peking University, Beijing, China. He also holds a joint appointment with the National Engineer-

ing Laboratory for Big Data Analysis and Applications, Peking University. Prior to joining PKU, he was a Postdoctoral Fellow with the ECE and ME Departments, Johns Hopkins University. His research interests include control, optimization, reinforcement learning, and market mechanisms, with application to power and energy systems.



Yan Jiang received the B.Eng. degree in electrical engineering and automation from the Harbin Institute of Technology, Harbin, China, in 2013, the M.S. degree in electrical engineering from the Huazhong University of Science and Technology, Wuhan, China, in 2016, and the M.S.E. degree in applied mathematics and statistics, in 2021, and the Ph.D. degree in electrical engineering from Johns Hopkins University, Baltimore, MD, USA, in 2021.

From 2021 to 2024, she was a Postdoctoral Scholar with the Department of Electrical and Computer Engineering, University of Washington, Seattle, WA, USA. She is currently an Assistant Professor with the School of Science and Engineering, The Chinese University of Hong Kong, Shenzhen, China. Her research interests include control, optimization, and learning, with application to power systems.



**Enoch Yeung** (Member, IEEE) received the B.S. degree in mathematics (magna cum laude with University Honors) from Brigham Young University, Provo, UT, USA, in 2010, and the Ph.D. degree in control and dynamical systems from the California Institute of Technology, Santa Barbara, CA, USA, 2016.

He is an Associate Professor with the Department of Mechanical Engineering, University of California, Santa Barbara. His research interests include learning algorithms for dynamical

systems, control theory, and control of biological networks.

Dr. Yeung was the recipient of the Kanel Foundation Fellowship, the National Science Foundation Graduate Fellowship, the National Defense Science and Engineering Fellowship, the PNNL Project Team of the Year Award, the PNNL Outstanding Performance Award, the Keck Foundation Award, the NSF CAREER Award, and an ARO Young Investigator Program Award.



Dennice F. Gayme (Senior Member, IEEE) received the bachelor's degree in mechanical engineering and society from McMaster University, Hamilton, ON, Canada, in 1997, the M.S. degree in mechanical engineering from the University of California, Berkeley, CA, USA, in 1998, and the Ph.D. degree in control and dynamical systems from the California Institute of Technology, Santa Barbara, CA, USA, in 2010.

She is currently a Professor of mechanical engineering with Johns Hopkins University, Bal-

timore, MD, USA. Her research interests include modeling, analysis, and control of spatially distributed and large-scale networked systems.

Dr. Gayme was the recipient of the JHU Catalyst Award in 2015, ONR Young Investigator and NSF CAREER awards in 2017, a Whiting School of Engineering Johns Hopkins Alumni Association Excellence in Teaching Award in 2020, and the Turbulence and Shear Flow Phenomena (TSFP12) Nobuhide Kasagi Award in 2022. She is a Fellow of the American Physical Society (2024) and the Standing Chair of the Women in Control Committee of the Control Systems Society of IEEE.



Enrique Mallada (Senior Member, IEEE) received the B.S. degree in telecommunications degree from Universidad ORT, Montevideo, Uruguay, in 2005, and the Ph.D. degree in electrical and computer engineering with a minor in applied mathematics from Cornell University, Ithaca, NY, USA, in 2014.

Prior to joining John Hopkins University, Baltimore, MD, USA, in 2016, he was a Postdoctoral Fellow with the Center for the Mathematics of Information, Caltech from 2014 to 2016. He is

currently an Associate Professor of electrical and computer engineering with Johns Hopkins University. His research interests include the areas of control, dynamical systems, and optimization, with applications to engineering networks, such as power systems and the Internet.

Dr. Mallada was the recipient of the NSF CAREER Award in 2018, the ECE Director's PhD Thesis Research Award for his dissertation in 2014, the Center for the Mathematics of Information Fellowship from Caltech in 2014, and the Cornell University Jacobs Fellowship in 2011.